Heliyon 10 (2024) e24330

Contents lists available at ScienceDirect

Heliyon

journal homepage: www.cell.com/heliyon

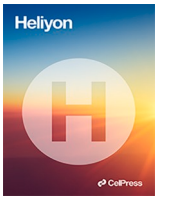

Review article

Whether membranes developed for organic solvent nanofiltration (OSN) tend to be hydrophilic or hydrophobic? —— a review

Yi-Hao Tong [b,1], Li-Han Luo [b,1], Rui Jia [b], Rui Han [b], Sun-Jie Xu [a,b,c,*], Zhen-Liang Xu [b,c]

[a] School of Materials Science and Engineering, East China University of Science and Technology, Shanghai 200237, China
[b] State Key Laboratory of Chemical Engineering, Membrane Science and Engineering R&D Lab, Chemical Engineering Research Center, School of Chemical Engineering, East China University of Science and Technology, Shanghai 200237, China
[c] Shanghai Electronic Chemicals Innovation Institute, East China University of Science and Technology, Shanghai 200237, China

ARTICLE INFO

Keywords:
Organic solvent nanofiltration (OSN)
Hydrophilic
Hydrophobic
Industrial application

ABSTRACT

In the past few decades, organic solvent nanofiltration (OSN) has attracted numerous researchers and broadly applied in various fields. Unlike conventional nanofiltration, OSN always faced a broad spectrum of solvents including polar solvents and non-polar solvents. Among those recently developed OSN membranes in lab-scale or widely used commercial membranes, researchers preferred to explore intrinsic materials or introduce nanomaterials into membranes to fabricate OSN membranes. However, the hydrophilicity of the membrane surface towards filtration performance was often ignored, which was the key factor in conventional aqueous nanofiltration. The influence of surface hydrophilicity on OSN performance was not studied systematically and thoroughly. Generally speaking, the hydrophilic OSN membranes performed well in the polar solvents while the hydrophobic OSN membranes work well in the non-polar solvent. Many review papers reviewed the basics, problems of the membranes, up-to-date studies, and applications at various levels. In this review, we have focused on the relationship between the surface hydrophilicity of OSN membranes and OSN performances. The history, theory, and mechanism of the OSN process were first recapped, followed by summarizing representative OSN research classified by surface hydrophilicity and types of membrane, which recent OSN research with its contact angles and filtration performance were listed. Finally, from the industrialization perspective, the application progress of hydrophilic and hydrophobic OSN membranes was introduced. We started with history and theory, presented many research and application cases of hydrophilic and hydrophobic OSN membranes, and discussed anticipated progress in the OSN field. Also, we pointed out some future research directions on the hydrophilicity of OSN membranes to deeply develop the effect made by membrane hydrophilicity on OSN performance for future considerations and stepping forward of the OSN industry.

* Corresponding author.
E-mail address: chemmembrxsj@ecust.edu.cn (S.-J. Xu).
[1] Yi-Hao Tong and Li-Han Luo contributed equally to this work.

https://doi.org/10.1016/j.heliyon.2024.e24330
Received 5 September 2023; Received in revised form 2 December 2023; Accepted 7 January 2024
Available online 12 January 2024

1. Introduction

1.1. History and definition

Efficient separation processes, which account for 40–70 % of total expenses in the chemical and pharmaceutical industries, were crucial for reducing costs, improving profitability, and achieving economic and environmental sustainability [1]. Pressure-driven membrane separation processes offered the potential to greatly decrease energy usage and running expenses in comparison to conventional thermal separation techniques [2]. Membrane-based separation methods offered advantages over traditional processes, such as a smaller footprint, reduced costs, higher energy efficiency, and no need for phase change [3].

Nanofiltration (NF) was a membrane-based separation process with a defined molecular weight cut-off (MWCO) that enabled the selective separation and purification of compounds within the 200–2000 Da range, achieving 90 % rejection of the target molecules. NF membranes had pore sizes ranging from 0.5 to 2 nm and operated under pressures between 5 and 30 bar, enabling efficient separation based on molecular size and weight [4]. NF demonstrates excellent potential for precise separation of small molecules using size exclusion and electrostatic effects, particularly in water treatment applications, thereby facilitating the purification of drinking water [5,6]. There were over 3000 organic solvents that were widely utilized within the chemical industry, comprising 80–90 % of chemical consumption yet, traditional separation methods recovered less than 50 %, resulting in substantial wastage and environmental issues [3,7]. The economic and environmental pressures necessitated the recovery of expensive and harmful organic solvents, highlighting the importance of solvent extraction and solute purification techniques for the future sustainability of these industries [8]. Conventional separation methods such as filtration, precipitation, adsorption, and distillation were energy-intensive separation techniques that were complex to operate, costly, energy-intensive, and produce wastes that could have a serious impact on the environment [9]. Organic Solvent Nanofiltration (OSN) or Solvent-Resistant Nanofiltration (SRNF) was an extremely energy-efficient alternative method for achieving precise nanoscale separations in severely aggressive and abrasive non-aqueous environments by applying pressure to membranes [10].

In 1964, Sourirajan first proposed the concept of OSN, employing cellulose acetate membranes for the effective separation of liquid hydrocarbon mixtures [11]. Loeb et al. proposed a pressure-driven membrane separation technology in 1965. In the following 20 years, cellulose acetate membrane became the dominant choice for OSN, while NF, introduced in 1984, filled the gap between ultrafiltration (UF) and reverse osmosis (RO) by selectively rejecting species based on their pore size [1]. During the 1980s, Exxon, Shell, and Union Carbide filed a significant number of patents for the filtration of organic solvents, showcasing a multitude of unique inventions in this domain [12]. Koch Membrane Systems brought polydimethylsiloxane-based membranes for OSN to the market during the 1990s [13]. In 1994, Mobil's Max-Dewax™ process incorporated polyimide (PI) as a crucial element, establishing itself as the world's biggest equipment during that period [13]. In 2007, See Toh et al. achieved the first-ever preparation of OSN membranes by chemically crosslinking integrally skinned Lenzing P84 polyimide membranes with aliphatic amine compounds [14]. In 2010, Jimenez et al. utilized interfacial polymerization (IP) to create innovative thin film composite (TFC) OSN membranes with improved solvent permeability compared to integrally skinned asymmetric (ISA) OSN membranes, while maintaining high rejection rates [15]. Recent efforts about OSN have been mostly focused on improving solvent resistance and pollution resistance.

2. Theory and mechanism

Three models describes the transport process through the membrane. Firstly, a model originated from irreversible thermodynamics treats the membrane to be like a "black box" without considering any properties of the membrane. Secondly, the other two models (belonging to the mechanistic model category) describes the solute transport according to structural and physicochemical parameters and takes into account the attributes of the membrane. These models includes the solution-diffusion model and the pore flow model [16–18]. Furthermore, hybrid transport mechanisms, incorporating features of both pore flow and solution-diffusion, have been suggested, exemplified by the model known as solution-diffusion with imperfections [19].

The selection of the optimal mechanical model category for a particular membrane is contingent upon its physical structure, distinguishing between porous and dense membranes. Investigating the connection between structure and performance enables a more profound comprehension of membrane permeation. The mathematical representations of permeation in solution-diffusion, pore flow, and solution-diffusion with defects models vary. These distinctions manifest in the factors considered for transport's driving forces and the quantity of model parameters that must be fitted or derived from independent measurements.

2.1. Irreversible thermodynamics model

Irreversible thermodynamics-based models characterize transport as an ongoing, non-reversible process that consumes free energy while generating entropy. The Kedem–Katchalsky model and the Spiegler–Kedem model, among the initial models rooted in irreversible thermodynamics, were the first ones employed for ion transport in NF membranes [20–22]. In accordance with irreversible thermodynamics, this process is delineated by phenomenological equations, treating the membrane as a 'black box' and omitting the depiction of its structure and electro-properties.

In terms of the Kedem–Katchalsky model, the solvent velocity (V), and the solute flux (J_i), are calculated by the following equations [20]:

$$V = Lp(\triangle p - \sigma i \triangle \pi) \tag{1}$$

$$Ji = Pi \triangle ci + (1 - \sigma i)V\overline{ci} \tag{2}$$

L_p is the mechanical filtration coefficient of the membrane, which also called local permeability coefficient, σ_i stands for the reflection coefficient, representing the portion of solute rejected by the membrane, and P_i is the permeability coefficient of the solute i. $\overline{ci}$ refers to the mean solute concentration within the membrane.

On the basis of the Spiegler–Kedem model, the solute flux is [21].

$$Ji = -Pi \triangle x\frac{\mathrm{d}ci}{\mathrm{d}x} + (1 - \sigma i)V\overline{ci} \tag{3}$$

The experimental rejection versus flux data is used to determine the permeability coefficient (P_i) and reflection coefficient (σ_i) for species i, through fitting with the following equation:

$$Ri = \frac{(1 - F)\sigma i}{1 - F\sigma i} \tag{4}$$

$$F = \exp[-V(1 - \sigma i) / \overline{Pi}] \tag{5}$$

$$\overline{Pi} = Pi/l \tag{6}$$

l is the membrane thickness along the radial coordinate x. In the Kedem–Katchalsky and Spiegler–Kedem models (Equations (2) and (3)), the first and second terms of the equations represent the contributions of diffusion and convection, respectively. Both these terms can be separately quantified and compared. This model is applicable to various solute and solvent systems, with σ_i and P_i derived from experimental data on solute and solvent fluxes. However, it is crucial to specify the solute (J_i) and solvent (V). For mixtures with n solutes, the irreversible thermodynamics model can be expanded to calculate the local solute permeation coefficient (P_i, where i = 1,2, … n) for each solute [23]. However, it is currently unclear how to extend this model to solvent mixtures or how to use it when solute and solvent can not be predetermined.

Through the introduction of the 'rational osmotic coefficient', this model can be extended to non-ideal mixtures. This coefficient is regarded as the ratio of the actual osmotic pressure to the osmotic pressure calculated using the van't Hoff formula (Equation (7)) and osmotic pressure is distinguished as in eq (8) [21]:

$$g = \frac{\pi}{vRTci} \tag{7}$$

$$\frac{\mathrm{d}\pi}{\mathrm{d}x} = vRT\left(g\frac{\mathrm{d}ci}{\mathrm{d}x} + ci\frac{\mathrm{d}g}{\mathrm{d}x}\right) \tag{8}$$

2.2. Models on concentration and pressure gradients

The category of models considers the properties of the membrane when describing the chemical potential gradients. The chemical potential gradient represents the overall driving forces that cause the permeate to move through the membrane [22]. The flux, J_i, of the component i, is

$$Ji = -Li\frac{\mathrm{d}\mu i}{\mathrm{d}x} \tag{9}$$

where μ_i represents the total chemical potential of species i, and L_i represents the proportionality coefficient between the flow rate and the driving force. μ_i is composed of the chemical potential dependent on pressure, temperature, and concentration, as well as the

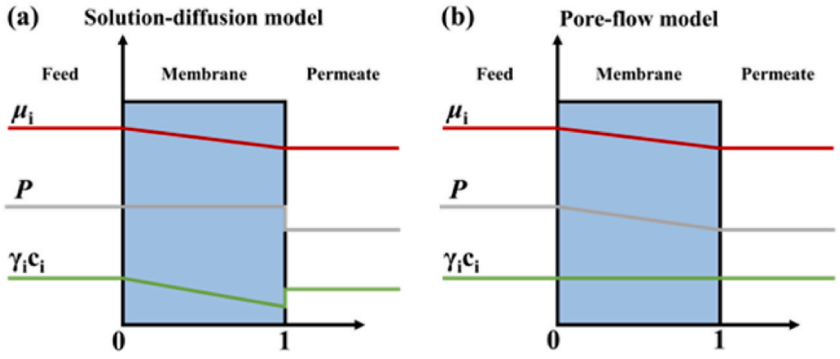

Fig. 1. Chemical potential, pressure, and solvent activity profiles are depicted for the pressure-driven filtration of a single-component solution through a membrane using (a) solution-diffusion and (b) pore-flow models.

electrochemical potential dependent on the electric potential. In processes involving multiple driving forces, such as reverse osmosis (RO) and nanofiltration (NF), this unified approach has proven to be very valuable. When only considering the concentration and pressure gradient, the chemical potential can be simplified as:

$$\mathrm{d}\mu i = RT\mathrm{d}\ \ln(\gamma ixi) + vid p \tag{10}$$

where x_i and v_i are defined as the molar fraction and the molar volume of species i, γ_i is the activity coefficient, and p is the pressure. The equation is able to be further simplified for incompressible phases:

$$\mu i = \mu_i^0 + RT\ \ln(\gamma ixi) + vi(p - pi, sat) \tag{11}$$

In the above equation, μ_i^0 is the chemical potential of pure species i under the saturation vapor pressure, $p_{i,\ sat}$.

Assuming there is a continuous chemical potential gradient from one side of the membrane to the other, this is due to the equilibrium reached between the fluid and solute at the interface. The solution-diffusion model and the pore-flow model characterize the chemical potential differently (Fig. 1): The former operates on the premise that the chemical potential gradient was concentration-dependent (Fig. 1(a)), whereas the latter posits that the chemical potential inside the membrane hinges on the pressure gradient (Fig. 1(b)).

2.2.1. Solution-diffusion model

Lonsdale et al. [16], Meares et al. [24], and Yasuda and Peterlin [25] introduced the solution-diffusion model, which is later reported by Mason and Lonsdale [26], and Wijmans and Baker [17] in the 1990s. This model exclusively delineates the chemical potential gradient within the membrane as a concentration gradient. It has found extensive application in elucidating transport phenomena in reverse osmosis, dialysis, pervaporation, and gas permeation processes [17].

The solution-diffusion model, commonly applied to characterize transport through dense membranes, posits that the fluxes of solute and solvent are mutually independent. This model suggests that the movement of permeants through the membrane aligns with the statistical fluctuations of free volume elements. It's important to note that these free volume elements should not be confused with pores, as the latter are generally considered to be stationary both in time and location.

When pressure gradient does not exist across the membrane, the solute flux is expressed as follows:

$$Ji = -Di\frac{\mathrm{d}ci}{\mathrm{d}x} = -\frac{RTLi}{ci}\frac{\mathrm{d}ci}{\mathrm{d}x} \tag{12}$$

Equation (12) bears resemblance to Fick's law, with the term RTL_i/c_i denoted as the diffusion coefficient D_i.

Conversely, in the presence of a pressure gradient across the membrane, the resulting equation for the 'classical solution-diffusion' model, upon integration over the membrane thickness, is:

$$Ji = \frac{DiKi}{l}\left[ci, 0 - ci, le^{-vi(p_0 - p_l)/RT}\right] = Pi\left[ci, 0 - ci, le^{-vi(p_0 - p_l)/RT}\right] \tag{13}$$

K_i is regarded as the sorption coefficient of species i.

Equation (13) is applicable to both solute (i) and solvent (V) fluxes across the membrane concerning pressure and concentration. In the case of diluted solutions, eq (13) can be streamlined for the solvent flux:

$$JV = \frac{DVKVcV, 0}{l}\left(1 - e^{-vV(\triangle p - \triangle \pi)/RT}\right) \tag{14}$$

where $\Delta\pi = \pi_0 - \pi_l$ is the differential osmotic pressure, which can be calculated by the van't Hoff equation [27]:

$$\triangle \pi = vRT(ci, 0 - ci, l) \tag{15}$$

If $(v_V(\Delta p - \Delta\pi))/(RT)$ is small, the solvent and solute fluxes becomes:

$$JV = \frac{DVKVcV, 0}{l}\frac{vV(\triangle p - \triangle \pi)}{RT} = LV(\triangle p - \triangle \pi) \tag{16}$$

$$Ji = \frac{DiKi}{l}(ci, 0 - ci, l) = Pi \triangle ci \tag{17}$$

where L_V and P_i are identified as the solvent and solute permeability coefficients, respectively.

Equations (16) and (17) are known as the 'simplified solution-diffusion' model. Paul evaluates the limitations of this model in the context of NF [28]. The solution-diffusion theory is inadequate for describing the separation of diverse organic systems due to its inability to consider any coupling between solute and solvent fluxes. The simplified solution-diffusion model predicts a linear increase in flux with pressure (Equation (16)), which contradicts experimental observations at high pressures. Moreover, the model overlooks the selective filtration of the membrane, and it fails to explain the negative rejection phenomena observed in specific solute-solvent systems [29]. These limitations stem from the model's neglect of the impact of pressure on solute transport. While this might be available for desalination processes, the model falls short in the presence of certain organic solutes or other solvents [28].

The "classical solution-diffusion" model (Equation (13)) doesn't need specifying which species is the solute and the solvent in

advance, allowing easy extension to multicomponent mixtures. On the other hand, the “simplified solution-diffusion" model distinguishes between solute (J_i) and solvent (J_V), and its expansion to solvent mixtures is not easy. By incorporating activity coefficients, the solution-diffusion model can be extended to non-ideal mixtures, as shown in Equation (11).

2.2.2. Pore-flow model

The pore flow model is on the basis of the assumption that transport through the membrane occurs by the way of permeation pathways (pores), which are much larger than the molecular diameters of the solute and solvent. Within these pores, the concentration of the solute and solvent is consistent. These models elucidate the chemical potential gradient across the membrane arising from a pressure gradient [22]. When there is no concentration gradient, the transport through porous membranes can be described using Darcy’s law:

$$Ji = k\frac{p_0 - p_l}{l} \tag{18}$$

k is the permeability coefficient while l is the membrane thickness. K is regarded as a function of structural factors, which could be pore size, surface porosity, and tortuosity, for instance.

The flux of a pure solvent moving through uniform cylindrical pores, in the absence of a substantial concentration gradient across the membrane, is articulated by the widely recognized Hagen–Poiseuille equation:

$$Jv = \frac{\varepsilon r p^2}{8l\tau}\frac{\triangle p}{\eta} = KHP\frac{\triangle p}{\eta} \tag{19}$$

In Equation (19), V is defined as the solvent velocity through the membrane pores.

When it comes to this simplified model, viscosity (η) is the sole solvent parameter influencing permeation. The membrane is characterized by pore size (r_p), porosity (ε), tortuosity (τ), and membrane thickness (l).

Regarding solute flux, several empirical models have been put forward to explain pore flow. Among them is the pore-flow model, which aims to elucidate the reflection coefficient in relation to pore radius. This concept is grounded in the irreversible thermodynamic model. Prominent models within this category encompass the Steric Hindrance Pore (SHP) model, Ferry model, Verniory model, and Log-Normal model. In the SHP model, the reflection coefficient is influenced by both the assumed uniform size of the membrane pore and the diameter of the solute [30]. Solute transport is influenced by spatial constraints and interactions with the pore’s boundaries. The reflection coefficient is determined as follows:

$$\sigma i = 1 - HFSF \tag{20}$$

where

$$HF = 1 + \frac{16}{9}\lambda \tag{21}$$

$$SF = (1-\lambda)^2\left[2 - (1-\lambda)^2\right] \tag{22}$$

$$\lambda = \frac{di}{dp} \tag{23}$$

H_F, denoted as a “wall-correction parameter," characterizes the impact of the pore wall, while S_F signifies steric hindrance within the pores. Here, d_i and d_p refer to the solute and pore diameters.

Ferry presents a pore-flow model to clarify the reflection coefficient, envisioning the pores as uniform and cylindrical, with the velocity demonstrating a parabolic profile within the pore [16]. The reflection coefficient is obtained through the following equation:

$$\sigma i = 1 - 2(1-\lambda)^2 - (1-\lambda)^4 \tag{24}$$

The Verniory model integrates frictional drag forces present in the cylindrical membrane pores, as represented by the factor g(λ) in eq (26) [31]. The equation expressing the reflection coefficient is as follows:

$$\sigma i = 1 - g(\lambda)SF \tag{25}$$

$$g(\lambda) = \frac{1 - (2/3)\lambda^2 - 0.2\lambda^5}{1 - 0.76\lambda^5} \tag{26}$$

2.3. Solvent-solute-membrane interaction

From the preceding paragraphs, it is clear that various interactions among solute, solvent, and the membrane plays significant roles in influencing molecular adsorption, exclusion, and permeation, alongside the primary driving forces in charge of transport across the membrane. The structural characteristics of the membrane combined with molecular interactions should be incorporated into transport models to be helpful to explain membrane transport and allow for the prediction of membrane performance. All these parameters are worthy of precise analysis.

Interactions between the solute, solvent, and membrane that influence the overall separation performance are categorized based on these factors: (i) the effective diameter of the solute; (ii) the pore wettability and effective diameter of the pores; (iii) the polarity of both the solute and solvent; and (iv) effects related to charge [32].

These interactions are schematically represented in Fig. 2.

3. Evaluation and measurements

3.1. Equipment and device

The permeability and selectivity performance of the OSN membrane are determined by solvent permeance and solute rejection. Permeance and solute rejection data are collected using dead-end stainless steel cells (Sterlitech HP4750) with a pressure of 5–21 bars, depicted in Fig. 3.

The performance of the OSN membrane and long-term filtration test can also be performed in the cross-flow filtration mode, which is shown in Fig. 4.

3.2. Pure solvent permeability

The volume of solvent that permeates the membrane per unit area and per unit time is known as the solvent flux, and the unit is L m^{-2} h^{-1}. Permeance, which is the flux per unit operating pressure and has a unit of L m^{-2} h^{-1} bar^{-1}, is typically used to standardize the flux at various operating pressures.

The flux (F, Lm^{-2} h^{-1}) is obtained by the following equation:

$$F = \frac{V}{A \times t} \tag{27}$$

V (L) represents the solvent volume of permeate, A (m^{-2}) represents the practical filtration area for each sample, and t (h) represents the filtration time.

The pure solvent permeance is determined using various organic solvents, and the permeance (P, L m^{-2} h^{-1} bar^{-1}) of each membrane is obtained by the subsequent equation:

$$P = \frac{V}{A \times t \times \Delta P} \tag{28}$$

Where V (L) is the volume of the permeate, t (h) is the filtration time, A (m^{-2}) is the practical area of each sample, and ΔP (bar) is the pressure on the membrane induced by the driving force of N_2.

3.3. Dyes removal ability

The filtration performance of the OSN membrane is evaluated using the solute rejection. It is calculated as the percentage ratio of solute able to be retained by the membrane to the total solute in the feed. Dyes, Active Pharmaceutical Ingredients (APIs), food components, and other solutes are frequently utilized in OSN investigations. Since different types of dyes have varying molecular

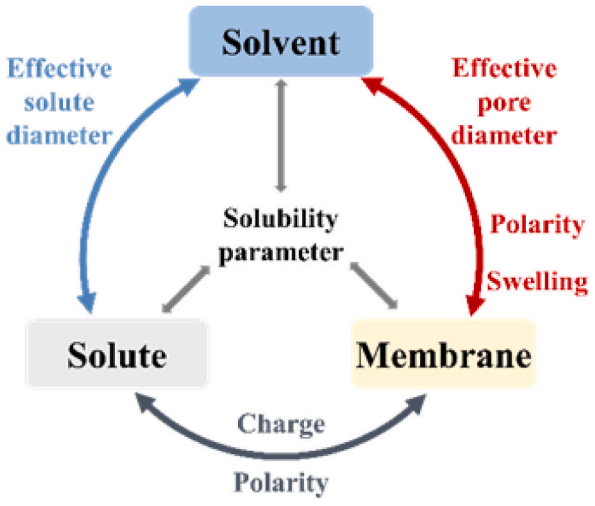

Fig. 2. Solute–solvent–membrane interactions affecting the overall separation performance. Effective Solute and Solvent Diameters and Polarity Effects.

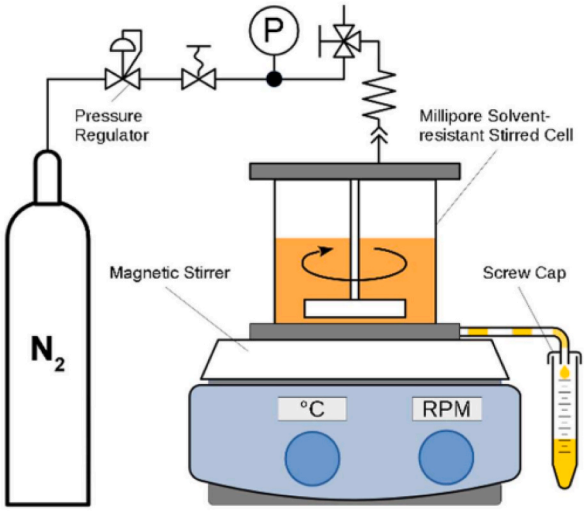

Fig. 3. Experimental setup of nanofiltration in a stirred cell [33].

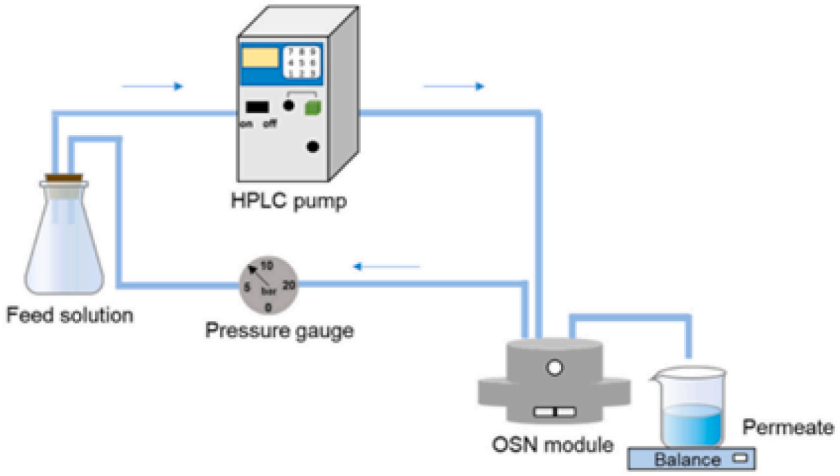

Fig. 4. Experimental setup of nanofiltration in a stirred cell [34].

weights which correspond to the test requirements for OSN membrane, dyes are used as solutes in the majority of studies. In contrast to other solutes, the dye concentration is also more easily determined by UV absorbance measurement.

The rejection (R, %) of the membranes is received using the subsequent equation:

$$R = \left(1 - \frac{C_P}{C_F}\right) \times 100\% \tag{29}$$

Wherein, C_P and C_F refer to the solute concentrations in the permeate and feed solutions.

3.4. Rejection curves

One of the most important OSN performance is the rejection curve of the membrane which reflect the rejection of each unit of the oligomers or polystyrene (PS), and polypropylene glycol (PPG). Some researchers also take aliphatic alkanes as the markers. The rejection values are obtained by analyzing the feeds and the permeate in terms of HPLC with C18 columns and calculating the peak area results.

3.5. Surface wettability

According to the pressure-driven membrane process, the wettability of membrane surfaces plays a crucial role in filtration per-

formance. The wetting properties of solid materials draw broad attention, and the OSN field is no exception. The wettability of the OSN membrane surface is usually measured through contact angles [35]. The relationship between contact angles and interfacial intension is proposed by Young's equation, which is put forward by T. Young in 1805 through mechanical analysis methods [36]. The equation reveals that when liquid contacted with a solid, the entire interface system is simultaneously subjected to the effects of gas-solid interface intension (also known as solid surface tension) γ_{sv}, gas-liquid interface tension (also known as liquid surface tension) γ_{lv}, and solid-liquid interface tension γ_{sl}, resulting in a specific contact angle of the liquid at the three-phase contact line of gas, liquid, and solid on the solid surface [37]. Fig. 5 exhibits the schematic image of a liquid on a horizontal solid surface.

$$\gamma_{lv} \cos\theta = \gamma_{sv} - \gamma_{sl} \tag{30}$$

Young's equation, also known as the wetting equation, is one of the oldest and most commonly equations in the field of physical chemistry, applied to the surface of materials. The interface field holds a very important position. It is not only the basis for quantifying the surface wettability of materials but also for calculating the surface tension and solid-liquid interface tension of solid materials through contact angles. From the equation, it can be seen that the moisture on the material surface. Wetness is closely related to liquid surface tension, solid-liquid interface tension, and solid surface tension. In the OSN field, the relationship between contact angle and OSN filtration performance has not been established. Commonly, researchers chooses the appropriate test systems according to the hydrophilicity of the OSN membrane or customized the surface properties of the OSN membrane according to the target systems. The review aims to list and summarize some OSN studies to establish the relationship between hydrophilicity and filtration performance.

4. Materials and structures

According to the materials of OSN membranes, it could be divided into polymeric materials and inorganic materials. Compared with traditional NF membranes, the materials of OSN membranes must meet more needs, which mainly included the following features: film-forming abilities, good chemical stability, appropriate cost and availability, well filtration performance, and so on. Generally, the majority of OSN membrane was polymer-based membrane. However, polymeric membranes had an obvious disadvantage in that they had inevitable performance reduction through long-term compaction and membrane fouling. In contrast, the inorganic membrane was advantageous in mechanical, thermal, and chemical stability. It not only could not swell or compact under harsh conditions but also was easy to clean. But Harder to up-scale and more britter restricted its wide application. Also, it was relatively unapproachable for inorganic materials to reach low MWCO and small-scale separation. The disadvantages of inorganic membranes were usually the advantages of organic membranes [32]. The choices of materials and modifications often influence the surface hydrophilicity of nanofiltration membranes. Traditional aqueous nanofiltration usually requires a relatively hydrophilic surface of a nanofiltration membrane. How to modify the aqueous nanofiltration membrane to make it more hydrophilic has become a mainstream direction researched by scholars. However, in OSN fields, rare researchers paid their attention to it. This section would simply classify representative studies on hydrophilic and hydrophobic OSN membranes, making brief introductions. Fig. 6 showed the classification of OSN membranes.

4.1. Hydrophilic OSN membrane

4.1.1. Hydrophilic ISA OSN membrane

In terms of ISA OSN membranes, polyimide was the most widely applied material of OSN membranes. Several years ago, researchers utilized polyimide to prepare OSN membranes directly through phase separation and cross-linking. In recent studies, it is often used as OSN support for further modification. In Fig. 7(a–d), schematic illustrations of some typical hydrophilic ISA OSN membranes was shown. Polyimide had some noticeable physicochemical properties [1] (e.g. high glass transition temperatures, Tg,

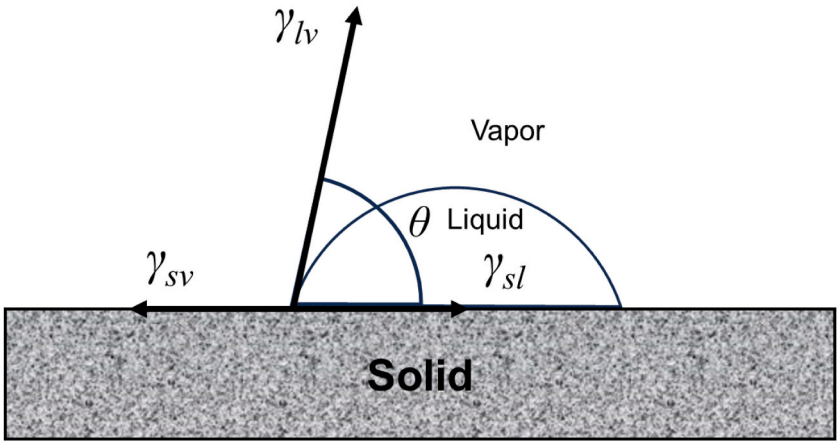

Fig. 5. Schematic of a liquid on a horizontal solid surface.

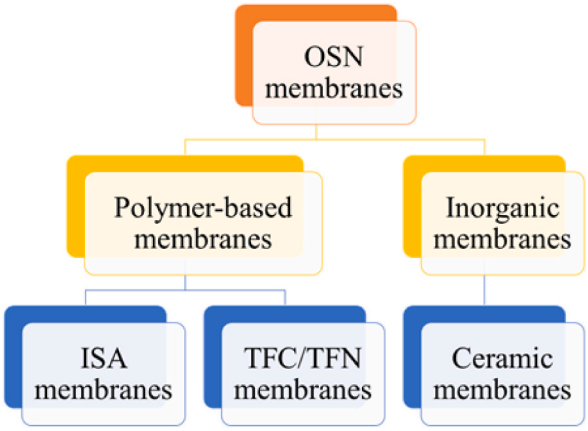

Fig. 6. Classification of OSN membrane.

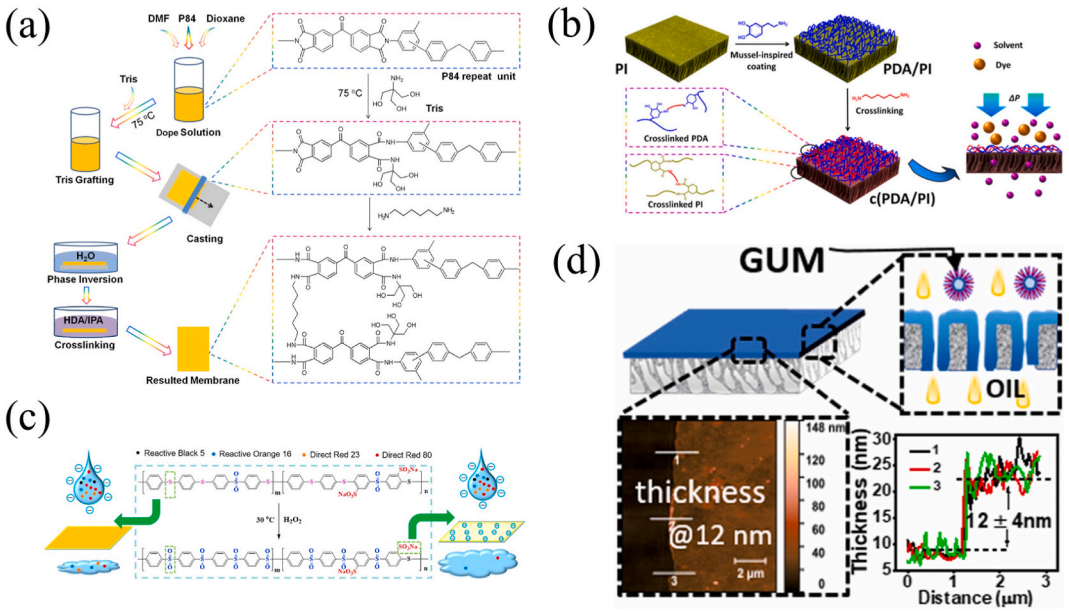

Fig. 7. Schematic illustrations of some typical hydrophilic ISA OSN membranes. (a) P84 OSN membrane grafted tris. Ref [38]. Copyright 2016, reproduced with permission from Elsevier B.V. (b) Polydopamine coating polyimide OSN membrane. Ref [39]. Copyright 2017, reproduced with permission from American Chemical Society. (c) Oxidization polyarylene thioether sulfone/sulfonated sulfone copolymers. Ref [50]. Copyright 2020, reproduced with permission from Elsevier B.V. (d) Crosslinked polyvinyl alcohol films. Ref [47]. Copyright 2022, reproduced with permission from Elsevier B·V.

good thermal and chemical stability). The above-mentioned good properties made it a desirable material for OSN membranes. Lenzing P84 was a representative co-polyimide, which was consistent with BTDA/TDI and BTDA/MDI with a composition of 80/20 % [2]. It has become a research hotspot in preparing OSN membranes. Xu et al. utilized a monoamine, tris(hydroxymethyl) aminomethane to modify the P84 membrane. P84 OSN membrane grafted by tris was more hydrophilic with a 270 % increase in IPA permeance [38]. In addition, polydopamine, as a hydrophilic nano glue, was widely applied in membrane modifications. Shao et al. prepared a polydopamine-coated polyimide OSN membrane and crosslinked it with hexamethylenediamine. The OSN membrane showed an ethanol permeance of 0.91 L m^{-2} h^{-1}·bar^{-1} and an RB rejection of 99 % [39]. Besides polyimide OSN membrane, polybenzimidazole was another usual polymer material, which attracted a lot of researchers to conduct studies [40–42]. Adam et al. grafted PEG and PPG on the PBI OSN membrane. Hydrophilic PEG graft modification could provide an effective method to reduce fouling during the OSN process [43].

ISA OSN membranes made from other polymeric materials and hydrophilic modification were also reported. El-Gendi et al. synthesized a novel polyetherimide, co-polyalkoxyetherimide, to prepare asymmetric OSN membranes. It exhibited better performance including higher rejection and flux than commercial polyimide, Kapton™ due to its hydrophilic nature [44]. Volkov et al. modified

poly (1-trimethylsilyl-1-propyne) (PTMSP) through plasma treatment and further research transport characteristics of various solvents and solutes [45]. Recently, some novel polymer was used to prepare OSN membrane. Jin et al. synthesized polyarylene thioether sulfone/sulfonated sulfone copolymers and fabricated OSN membrane via the non-solvent induced phase separation (NIPS) method. Subsequent oxidization and molecular design could improve the hydrophilicity of the membrane and keep it stable in N-methyl-2--pyrrolidone (NMP) [46]. This oxidization process also enhanced both rejection (by 85.2 %) and permeability (by 105 %). Thummer et al. fabricated polyvinyl alcohol (PVA) nanofilm and crosslinked with maleic acid on poly (acrylonitrile-*co*-methacrylic acid) substrate, which was resistant the various solvents. The resultant membrane could applied in specific separation of phospholipid with flux of 14 L m^{-2} h^{-1}·bar^{-1} and phospholipid rejection selectivity of 92 %, which showed potential in degumming of crude vegetable oil [47]. Beyond that, some water-soluble materials could be considered including sodium alginate [48], chitosan [49], and so on. These materials had potential to prepare OSN membranes after certain modifications.

4.1.2. *Hydrophilic MMMs OSN membrane*

To reach certain separation requirements and selectivity, ISA OSN membranes often needed crosslinks. However, the crosslinking method tended to cause the permeance decline. To improve the filtration performance, various inorganic fillers were added to polymer matrices to prepare mixed matrix membranes (MMMs). Silica, zeolites, metal organic frameworks (MOFs), covalent organic frameworks (COFs), graphene oxide [51,52], carbon nanotubes (CNTs), and some other fillers were researched in OSN membranes [53,54]. It was worth mentioning that immobilized nanoenzymes had a big application in various field including food industry [55,56], environmental modification [57,58], and so on. Its application in mixed matrix OSN membranes was worth looking forward to. MMMs were able to scale up easily and enhance solvent resistance, mechanical properties, thermal stability, and so on with the introduction of inorganic fillers. Schematic illustrations of some typical hydrophilic MMMs OSN membranes were shown in Fig. 8(a–d). Farahani et al. blended amine-functionalized multi-walled carbon nanotubes (NH_2-MWCNTs) with P84 polymer to prepare MMMs through the NIPS method. The introduction of NH_2-MWCNTs could enhance the porosity, sorption capacity, and liquid transport of MMMs, the resultant membranes had high alcohol permeances of ethanol and isopropanol and showed a good rejection of 92.1 % to tetracycline, which had potential application in separation active pharmaceutical ingredients (APIs) [59]. Gao et al. developed a novel vapor-phase crosslink method by introducing Zr-based MOF UiO-66-NH_2. The optimal membrane had a 99.2 % rejection of RB with a pure isopropanol flux of 11.5 L^{-1} m^{-2} h^{-1} at 10 bar [59]. Si et al. utilize a silane coupling agent to modify MCM-41 to generate amine groups. Amine groups could crosslink with polyimide to open an imide ring, which could avoid forming the non-selective interfacial voids in the filler-polymer interface [60]. 5 wt% NH_2-MCM-41/Polyimide MMMs reached the 78 % and 131 % increment of ethanol and isopropanol flux without reduction of rejections. Besides adding microporous and mesoporous nanoparticles, 2D materials had also been widely applied in preparing OSN membranes recently. Shen et al. dispersed MXene by potassium fulvic acid to incorporate into the P84 matrix. Exfoliation with potassium fulvic acid avoids the use of toxic reagents, which made the fabrication process greener. U–Ti3C2Tx could promote the permeance of ethanol with a slight decrease in rejection to BBR [61]. Generally speaking, inorganic nanofillers could improve the surface roughness of the membrane, especially hydrophilic nanofillers. The surface of hydrophilic materials with

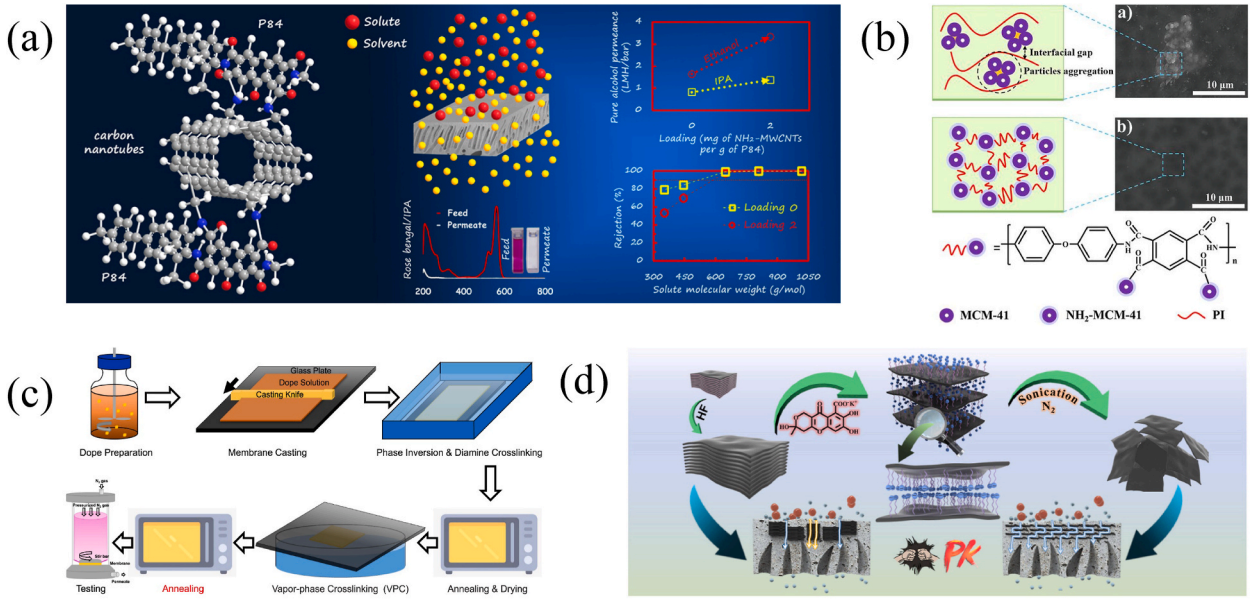

Fig. 8. Schematic illustrations of some typical hydrophilic MMMs OSN membranes. (a) NH_2-MWCNT crosslinked P84 OSN membranes. Ref [59]. Copyright 2018, reproduced with permission from Elsevier B.V. (b) NH_2-MCM-41/Polyimide MMMs. Ref [60]. Copyright 2020, reproduced with permission from Elsevier B.V. (c) Vapor-phase crosslinked polyimide OSN membranes. Ref [62]. Copyright 2019, reproduced with permission from Elsevier B.V. (d) U–Ti3C2Tx MMMs. Ref [63]. Copyright 2023, reproduced with permission from Elsevier B·V.

higher roughness could have lower contact angle and better hydrophilicity. The reverse is also true for hydrophobic OSN membranes.

4.1.3. Hydrophilic TFC/TFN OSN membrane

Different from ISA membranes, thin film composite (TFC) membranes of thin film nanocomposite membranes (TFN) are fabricated with ultrafiltration substrates and thin skin layers. So far, major of research on OSN membrane transferred from ISA OSN membrane to TFC/TFN OSN membrane [64]. In this study, interfacial polymerization (IP) was a key technique to prepare TFC/TFN membranes. Due to its relatively thin separation layer, the TFC/TFN membrane frequently had better filtration performance than the ISA membrane [65]. This kind of membrane with an ultrathin layer and porous support could be independently designed and constructed to meet the needs of complex target applications.

Sorribas et al. combined four MOFs with different particle sizes including ZIF-8, MIL-53(Al), NH2-MIL-53(Al), and MIL101(Cr) into a polyamide layer through IP. The addition of MOF could increase the flux due to the porosity of MOFs, which provided an extra pathway for solvent transport. These MOFs showed good compatibility during the combination of polyamide so the rejection of the as-prepared membrane had no significant decline [66]. Besides direct doping in the skin layer, the construction of the interlayer was another crucial strategy during OSN membrane preparation. Li et al. deposited ethylenediamine crosslinked graphene oxide on PI substrate, and then conducted PA through IP. The formed PA layer was ultrasmooth, ultrathin, hydrophilic, and detect-free. The TFN OSN membrane had 99.4 % rejection for rhodamine B with ethanol permeance of 4.15 L m^{-2} h^{-1}·bar^{-1}. Also, the membrane maintained stability in DMF for more than 160 days, which showed excellent solvent resistance [67].

Traditional IP utilized amine monomers and acyl chloride monomers to react in the interface between the water phase and the organic phase. With the development of IP, various aqueous monomers were researched. Liu et al. constructed the OSN skin layer via an interfacial reaction between cyclodextrin (CD) and trimethyl chloride (TMC). Hydrophobic inner cavities of CD benefited the permeance of nonpolar solvent while hydrophilic transport channels between CDs facilitated the mass transfer of polar solvent. The OSN membrane had a molecular sieving skin layer with Janus pathways that could better balance the trade-off effect during the OSN process [68]. Moreover, Jimenez Solomon et al. developed ultrathin crosslinked polyacrylate nanofilm membranes through IP with by rigid contorted monomers. Microporous polyacrylate network showed high solvent permeance and resistance in OSN. The microporous polymers explored a new kind of polymer material prepared by IP and showed great potential in molecular separation [69]. Schematic illustrations of some typical researches mentioned above were shown in Fig. 9(a–d).

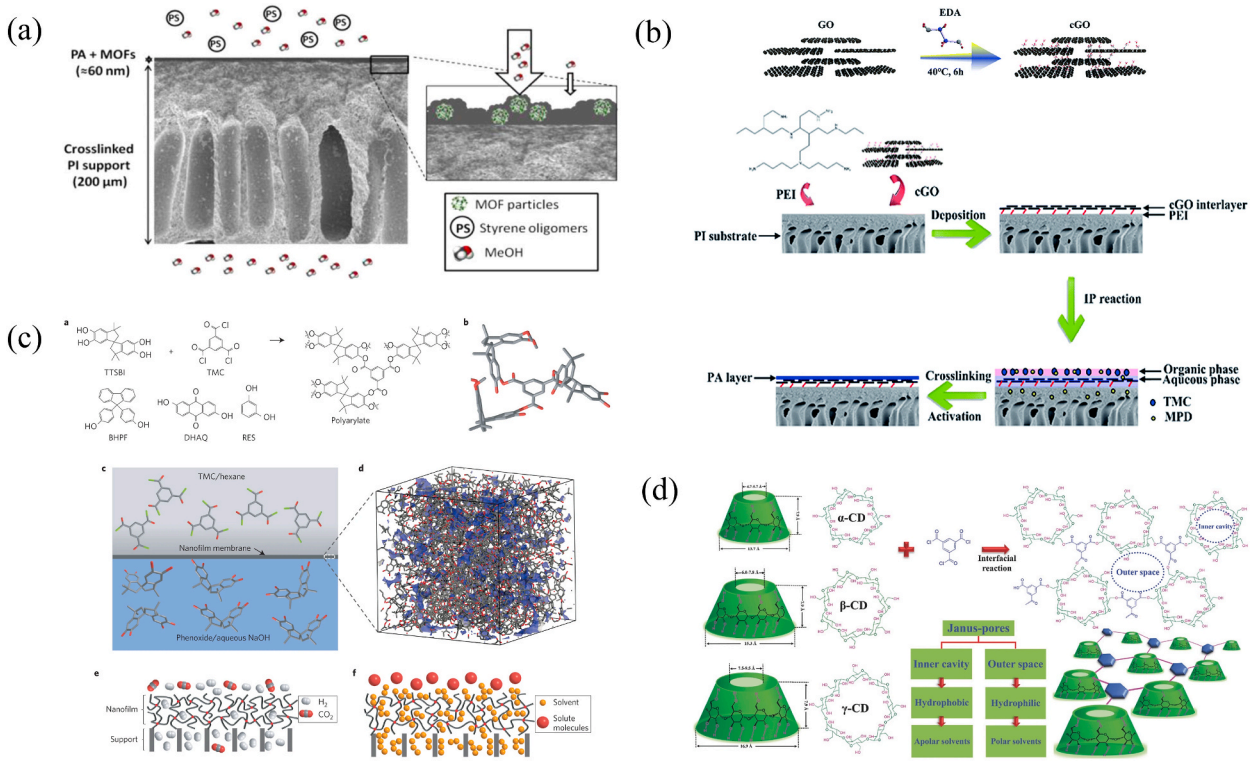

Fig. 9. Schematic illustrations of some typical hydrophilic TFC/TFN OSN membranes. (a) PA + MOFs. Ref [66]. Copyright 2013, reproduced with permission from American Chemical Society. (b) EDA crosslinked cGO. Ref [67]. Copyright 2019, reproduced with permission from Royal Society of Chemistry. (c) Ultrathin crosslinked polyacrylate nanofilm membranes. Ref [69]. Copyright 2016, reproduced with permission from Nature. (d) TFC OSN membrane prepared by CDs. Ref [68]. Copyright 2018, reproduced with permission from Wiley.

4.1.4. Others

Apart from traditional phase separation and IP methods, there were other facile methods to prepare OSN membranes such as vacuum filtration, layer-by-layer self-assembly, and so on. Schematic illustrations of relative researches were shown in Fig. 10(a–d). Wang et al. synthesized MoS_2 quantum dots (MQDs) and incorporated them into graphene oxide membranes via vacuum filtration on nylon porous substrates, which was inspired by the shell of the Namib Desert beetle. The heterostructured lamellar membrane had a dual-functional zone, which increases the flux of various solvents more than pure GO membrane, providing a promising method for constructing a 2D OSN membrane [70]. In terms of 2D membranes, changing d-spacing via small molecules was a common method [71], which could reach the controlled adjustment of lamellar transport channels. In addition, the modification of 2D nanosheets was also reported. Huang et al. prepared solvent-solvated rGO and deposited it on the microfiltration substrates. The OSN membrane not only kept stable in organic solvents but also showed good resistance to strong acids and bases. At the same time, high rejections to small molecules and high permeances to organic solvents were retained [72]. Polyelectrolyte multilayer (PEM) could be prepared by layer-by-layer self-assembly technique through electrostatic interactions. Due to its customized thickness and surface charge, PEM had a certain amount of research in OSN. Liang et al. deposited PSS/PDDA PEM on the hydrolyzed polyacrylonitrile and prepared the counterion-switched reversibly hydrophilic and hydrophobic surface respectively by loading TiO_2 and perfluorooctanoate. The membrane with a hydrophilic surface showed a low contact angle ($13.2° \pm 1.8°$), which could separate dyes in both aqueous and non-aqueous systems through the motion and interaction between the hydrophilic layer and hydrophobic layer [73].

4.2. Hydrophobic OSN membrane

According to applications of OSN, quite a few circumstances was faced with nonpolar solvent. In this particular case, a hydrophobic surface was preferred. Although the number of research on hydrophobic OSN membranes was inferior to that of hydrophilic OSN membranes, there were still some notable materials suitable to be applied in OSN such as PVDF (Polyvinylidene Fluoride), PTFE (Polytetrafluoroethylene), PDMS (Polydimethylsiloxane) and so on.

4.2.1. Hydrophobic ISA OSN membrane

As far as hydrophobic ISA membrane, PVDF was one of the most common materials that could prepare UF membranes via the NIPS method. To increase the solvent resistance, Mertens et al. utilized *p*-xylenediamine to crosslink PVDF. Rigid benzene-containing crosslinking agents could decrease the swelling of acetonitrile, dimethyl formamide, and toluene, and its acetonitrile permeance exceeded the majority of commercial membranes [74]. Despite hard to be long-term stable in strong polar aprotic solvents such as DMF, DMAc, DMSO, NMP, and so on, PVDF has great potential application in nonpolar solvents. Pagliero et al. prepared PVDF-Si and PVDF-CA two tailor-made flat composite membranes to separate sunflower oil from hexane, which had better performance than commercial MPF-50 membranes [75]. Besides the separation of sunflower oil, Firman et al. integrated the usage of lab-made PVDF

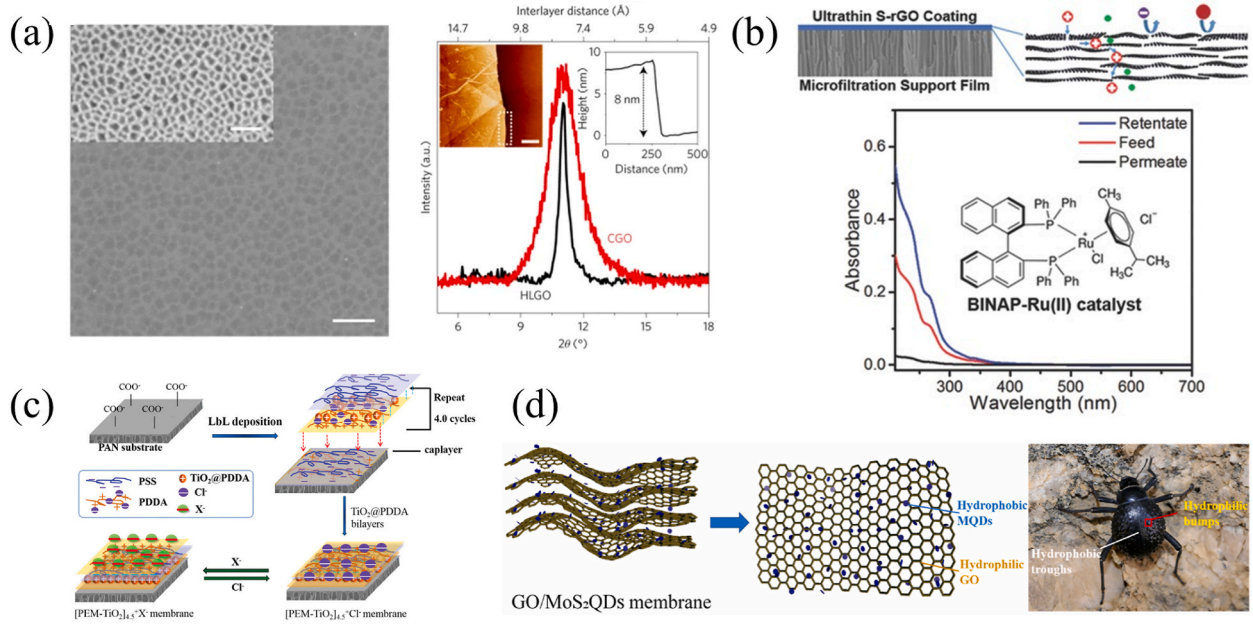

Fig. 10. Schematic illustrations of other typical hydrophilic membranes. (a) Ultrathin graphene-based membrane. Ref [71]. Copyright 2017, reproduced with permission from Nature. (b) Ultrathin S-rGO coated OSN membranes. Ref [72]. Copyright 2016, reproduced with permission from Wiley. (c) PSS/PDDA Polyelectrolyte membranes. Ref [73]. Copyright 2016, reproduced with permission from Wiley. (d) GO/MoS_2 QDs membranes. Ref [70]. Copyright 2022, reproduced with permission from Elsevier B·V.

membrane and Solsep 030 306 silicon-base polymer nanofiltration membrane on a single membrane multistage scheme for the recovery of soybean oil to replace the traditional evaporation process. This method could reach a reduction of 60 % consumption while saving 50 % energy requirements [76]. Schematics of some of the above researches were shown in Fig. 11(a–c).

4.2.2. *Hydrophobic MMMs OSN membrane*

Similar to hydrophilic MMMs OSN membranes, nanomaterials could directly modify hydrophobic OSN membranes via simple blending. The blend of PDMS and nanomaterials was a common strategy. Li et al. synthesized mesoporous silica particles and added them into PDMS OSN. The predominant pore size could be adjusted to 2.1 nm, which benefited the transport of various solvents with the removal of trace impurities, especially Evans blues and vitamin B12 [77]. Ji et al. controllably prepared siloxene/PVDF membrane via NIPS method. The incorporation of 2D siloxene nanosheets could induce the PVDF membrane to become highly compacted, have low free volume, and have good ordering, which could transfer the UF PVDF membrane into the NF PVDF membrane [78]. With the same hydrophilic OSN membrane, MOFs had a great deal of research work on hydrophobic MMMs. Different from relatively hydrophilic membrane materials, hydrophobic materials were hard to combine with MOFs due to poor adhesion between membrane materials and fillers. Basu et al. incorporated four trimethylsilyl-modified MOFs into PDMS matrix including $Cu_3(BTC)_2$, MIL-47, MIL-53(Al), and ZIF-8. As-prepared MMMs had a higher rejection in the RB/IPA system compared with the original membrane. MOFs could reduce the swelling effect of polymers and increase the size exclusion of dye molecules [79]. With the development of up-scaling production of nanomaterials like MOFs, large-loaded MMMs were gradually explored and researched. Karimi et al. prepared 25 wt% ZIF-8/PVDF MMMs Its excellent anti-compaction and reduced swelling degree made it well reject RB in the ethanol and IPA

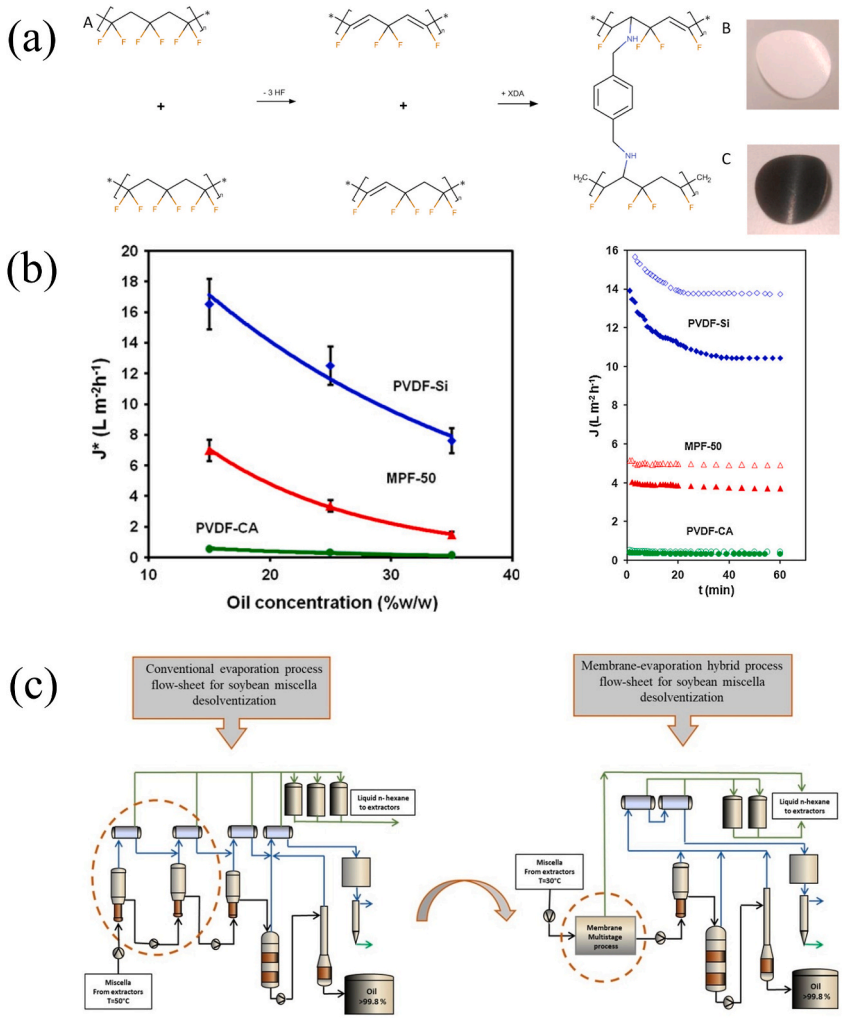

Fig. 11. Schematic illustrations of some typical hydrophobic ISA OSN membranes. (a) Crosslinked PVDF OSN membranes. Ref [74]. Copyright 2018, reproduced with permission from Elsevier B.V. (b) PVDF-Si and PVDF-CA membranes. Ref [75]. Copyright 2011, reproduced with permission from the American oil Chemists' Society. (c) A single membrane multistage scheme. Ref [76]. Copyright 2020, reproduced with permission from Elsevier B·V.

[80]. Diagrams of the relevant examples were shown in Fig. 12(a–d).

4.2.3. Hydrophobic TFC/TFN OSN membrane

When it came to hydrophobic TFC/TFN OSN membranes, the introduction of another special monomer was a common method. Solomon et al. first reported hydrophobic TFC membranes prepared through interfacial polymerization with fluorinated amine and acyl chloride. The filtration permeance of toluene and ethyl acetate of the TFC membrane was better than commercial OSN hydrophobic ISA membranes and rubber-coated membranes. The incorporation of F in the PA layer could improve the flux of nonpolar solvents. Such hydrophobic TFC OSN membranes prepared via IP and treated with DMF for post-activation could be possibly become the next generation of excellent OSN membranes [81,82]. Apart from the addition of reactible monomers during IP, the introduction of special macromolecules or polymers could also have a good modification effect. Mohamed et al. synthesized poly (divinylbenzene--*co*-perfluorodecyl acrylate) (poly (DVB-*co*-PFDA) nanoparticles through free radical precipitation polymerization. Different from hydrophobic monomers, such hydrophobic polymer particles could improve the permeance of both polar and nonpolar solvents without any decline of solute rejections. Appropriate loading offered versatility in the design and fabrication of such TFC OSN membranes [83]. Hydrophobic OSN membrane will have wide application in hydrocarbon separation in the future, due to it could reduce energy consumption. Li et al. prepared a hydrophobic TFC membrane via IP with self-assembled multiblock oligomer amines (MOAs). This process incorporated vesicles, which made the resultant membrane more permeable, selective, and stable. In application, the hydrophobic TFC membrane could manipulate the crude oil separation, which had better performance than commercial membranes and other literature reported [84]. So far, most research on OSN TFC membranes focused on hydrophilic membranes. The above-mentioned research and applications on hydrophobic OSN membranes could accelerate the development of the OSN technique. Schematic illustrations of above researches were shown in Fig. 13(a–c).

4.2.4. Other

Speak of hydrophobic OSN membrane, surface modification, and hydrophobic surface coating were a kind of methods that could be up-scaled. Kujiawa et al. grafted perfluoroalkylsilanes on ceramic membranes to form perfluoralkylsilane nanolayers. Titania ceramic membranes after grafting showed stability in chloroform and hexane, while the nanolayer had no obvious influence on the internal structure. This hydrophobic modification had good performance on air gap membrane distillation and pervaporation [85], which was helpful during preparing ceramic OSN membranes. In the polymeric membranes, Guo et al. utilized trimethylperfluorinatesilane (PFAS) to modify poly (ethylenimine)/poly (acrylic acid) (PEI/PAA)calcium silicate hydrate (CSH) multilayered membranes

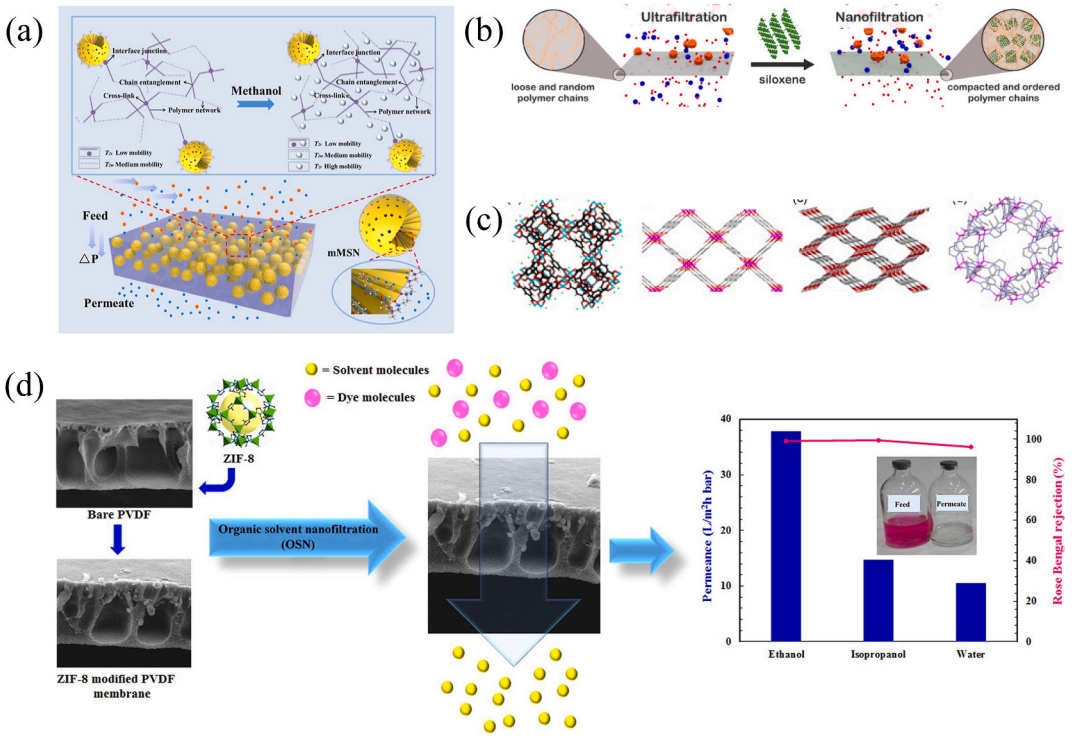

Fig. 12. Schematic illustrations of some typical hydrophobic MMMs OSN membranes. (a) mesoporous silica particles Ref [77]. Copyright 2020, reproduced with permission from Elsevier B.V. (b) Siloxene/PVDF membranes. Ref [78]. Copyright 2021, reproduced with permission from Elsevier B.V. (c) Trimethylsilyl-modified MOFs/PDMS membranes. Ref [79]. Copyright 2009, reproduced with permission from Elsevier B.V. (d) ZIF-8/PVDF MMMs. Ref [80]. Copyright 2020, reproduced with permission from Elsevier B·V.

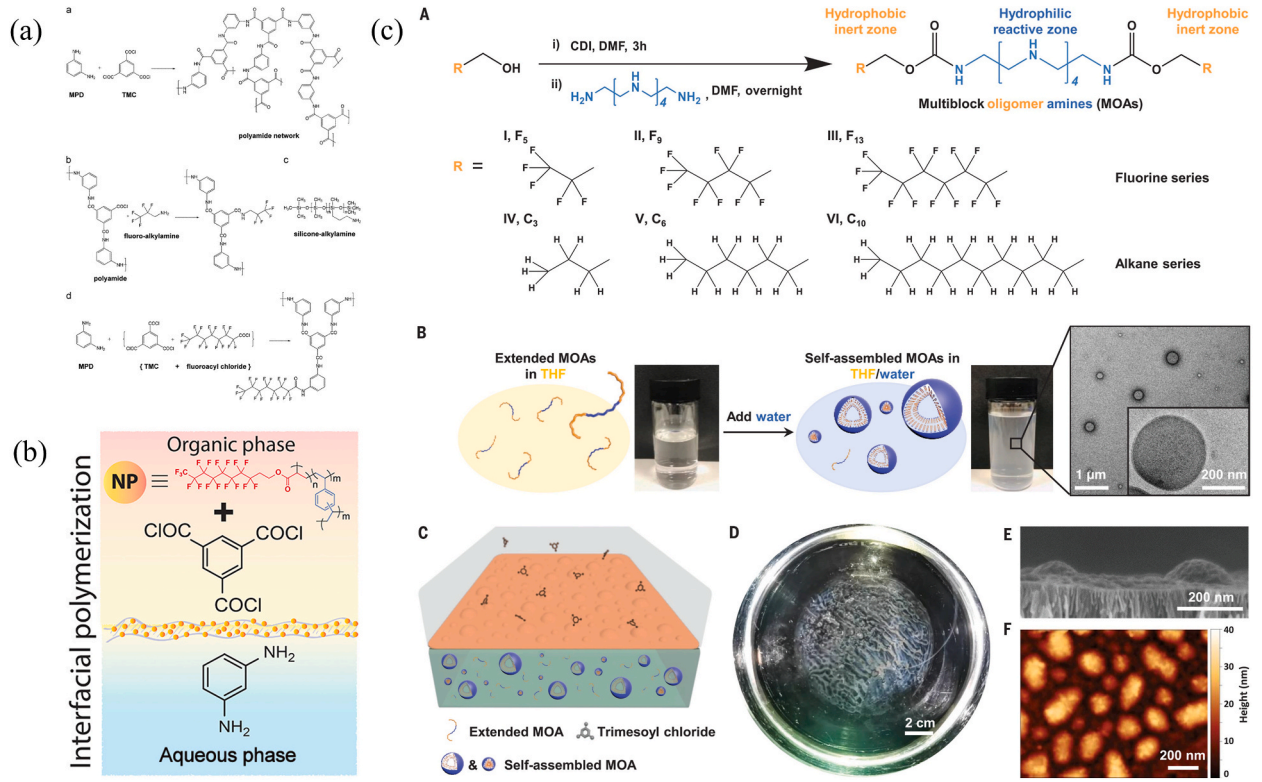

Fig. 13. Schematic illustrations of some typical hydrophobic TFC/TFN OSN membranes. (a) Hydrophobic TFC membranes prepared via IP with fluorinated amine and acyl chloride. Ref [82]. Copyright 2013, reproduced with permission from Elsevier B.V. (b) Poly (divinylbenzene-*co*-perfluorodecyl acrylate) (poly (DVB-*co*-PFDA) nanoparticles modified PA OSN membranes. Ref [83]. Copyright 2021, reproduced with permission from American Chemical Society. (c) Hydrophobic TFC membrane via IP with self-assembled multiblock oligomer amines (MOAs). Ref [84]. Copyright 2022, reproduced with permission from Science.

$(PEI/PAA\text{-}CSH)_n$ to form superhydrophobic OSN membrane. Such one-step modification could transform the wettability of the membrane surface which is applied to adapt to different external circumstances [86]. On the other hand, hydrophobic modification to nanoparticles could help them to combine with hydrophobic materials better. Li et al. modified attapulgite (ATP) through polystyrene (PS) grafting so that it was well compatible with the polyphenylene sulfide (PPS), which ATP-PS could conduct crosslink between PPS polymer chains to increase the mechanical properties of PPS membrane [87]. In a particular application, Chau et al. researched two kinds of perfluorinated membranes whose prefixes were 106 and 255.106 was an amorphous hydrophobic perfluorinated polymer supported by PAN substrates while 255 was made by hydrophilically perfluorinated polymer supported by expanded polytetrafluoroethylene (ePTFE). These two membranes were applied in a two-stage OSN process, achieving 99 %+ rejection to a 432 Da compound with long-term stability in a strong polar aprotic solvent such as DMSO, NMP, EtAc, and so on. Briefly, hydrophobic OSN also had broad prospects for development compared with hydrophilic OSN. Fig. 14(a–d) showed schematic illustrations of mentioned researches. Lab-scale research on OSN should consider practical applications so that OSN membranes were designed and tailored to fit the complex circumstances of application [88]. Table 1 summarized various OSN membrane preparation methods and their separation performance and contact angle data for easy reference (see Fig. 15).

5. Applications

Industries are increasingly drawn to OSN, a “green process,” for its minimal carbon emission, cost-effectiveness, gentle operating conditions, and efficient separation that minimizes waste [134]. OSN finds extensive applications across various industries including petrochemicals, food processing, bulk, and fine chemistry, as well as the pharmaceutical sector.

OSN, often referred to as a “green process," is garnering increasing attention from industries due to its multiple benefits. These include minimal carbon emission, cost-effectiveness, gentle operating conditions, and efficient separation that leads to reduced waste [134]. This technology has been extensively applied in diverse sectors such as petrochemicals, food processing, bulk and fine chemistry, and the pharmaceutical industry.

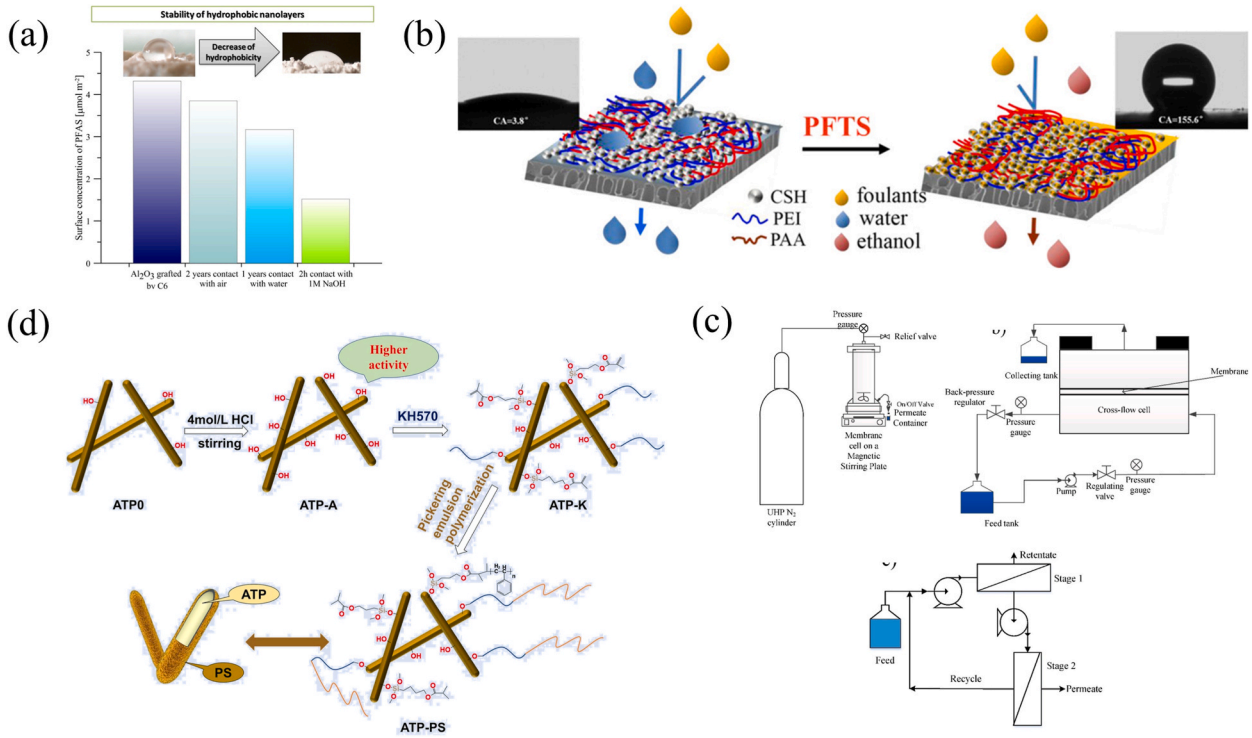

Fig. 14. Schematic illustrations of other typical hydrophobic OSN membranes. (a) Perfluoralkylsilane nanolayers membranes. Ref [85]. Copyright 2014, reproduced with permission from Elsevier B.V. (b) PFAS modified PEI/PAA multiplayer membranes. Ref [86]. Copyright 2016, reproduced with permission from American Chemical Society. (c) Two-stage OSN processes. Ref [88]. Copyright 2021, reproduced with permission from Elsevier B.V. (d) ATP-PS modified PPS membranes. Ref [87]. Copyright 2023, reproduced with permission from SpringerLink.

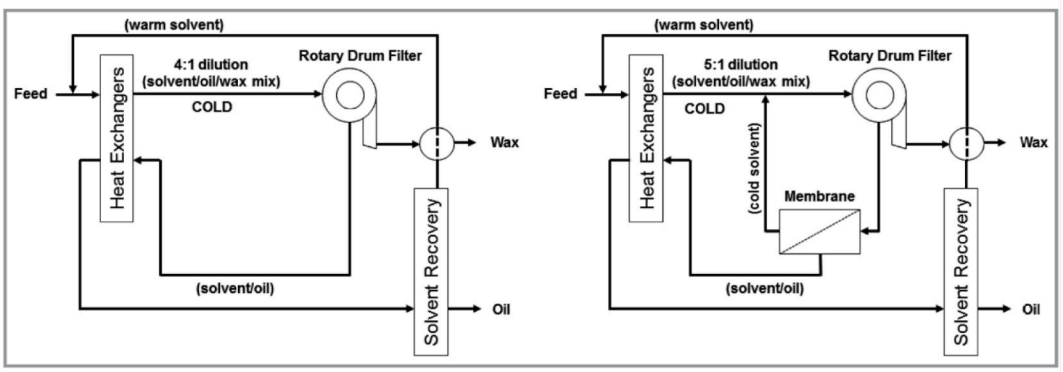

Fig. 15. Conventional solvent-based cold wax removal (left), Wax removal utilizing OSN (right) [13].

5.1. Petrochemical industry

5.1.1. Dewaxing of lube oil

Amongst the applications of OSN in the petrochemical sector, the Max-Dewax™ technique shines as the epitome of achievement, extracting dewaxing solvents from filtrates of lubricating oils. Exxon and Grace's collaboration has resulted in the development of an innovative OSN-based method that improves the efficiency of separating dewaxing solvents from lubricating oils. By using OSN membranes instead of the traditional evaporation step, the process was able to obtain solvent mixtures up to 99 % pure at low temperatures. The investment cost of using OSN was only one-third of the original cost, making it more cost-effective than conventional processes. In addition, the new process consumes only 25 % of the heat, 10 % of the cold, and 20 % of the volume compared to the conventional process. This improvement not only reduces energy consumption but also contributes to a quick payback, as the payback period was less than one year. This achievement marks a breakthrough in separation technology for the petrochemical

Table 1
Comparison of OSN filtration performances and its contact angles.

Membrane code	Method	Contact angle (°)	Filtration performance		Ref.
			Permeability ($L \cdot m^{-2} \cdot h^{-1} \cdot bar^{-1}$)	Rejection (%)	
PDMS-γ-Al_2O_3	Grafting	108	3.1 ± 0.1 (Tol) 4.5 ± 0.2 (EtOAc) 0.9 ± 0.1 (IPA)	45 ± 1 30 ± 1 20 ± 1 Sudan Black	[89]
[(PDDA/PAA-CSH)2.5]+PFO−	LBL assembly	118	5.4 (EtOH)	99.1 Methyl Blue	[90]
Crosslinked Alginate/PAN	Spin coating	25	1.27 (MeOH)	98 Vitamin B12	[3]
PA@PAN/PET	IP	79.2	4.5 (MeOH)	>94 CR	[91]
TTB-CMP	Electrochemical polymerization	92	21 (MeOH)	>90 500 Da	[92]
NF-3VA	Crosslink	86	4.5 (THF)	93 Crystal violet	[93]
TFC-aramid	IP	4.3	29.5 (MeOH)	84.4 Fast green	[94]
PA (TEPA-TCL)@PSU/PETP membrane	IP	78	1.5 (MeOH)	99.91 Congo Red	[95]
PA-COFs-c/PI	IP	72	8.0 (EtOH)	99.4 Rhodamine	[96]
BTDA + MDA-275	IP	62.3	11.2 (DMF)	99.7 Rose Bengal	[97]
PA/CaAlg-HKUST-16/PEI	IP	54.5	4.9 (EtOH)	94.7 Methyl blue	[98]
(PA/GQDs-100-PEI-500/PI)XA	IP	62	5.5 (EtOH)	98.7 Rhodamine B	[99]
AF2400/PTFE		114.8	1.1 (Hexane)	>98 oil	[100]
PA/ZIF-93/MWCNT/P84	IP	56	84.5 (MeOH)	99.8 Rose Bengal	[101]
PI-0.86-PA	IP	≈57	5.5 (MeOH)	99.6 G250	[102]
TFC–HFBC	IP	100	10 (Toluene)	87 Hexaphenylbenzene	[103]
PEK-SPEDEK	NIPS	71	16.3 (EtOH)	99.9 Rose Bengal	[104]
PpPD-TMC/HPAN	IP	53.6	242 (EtOH)	91.2 Congo Red	[105]
Phi–NF–2 (PA)	IP	43.6	2.6 (MeOH)	92.9 Erythrosin B	[106]
Pho–NF–2 (PA)		87.8	6.6 (THF)	99.5 Erythrosin B	
PA/HKUST-1/crosslinked P84	IP	39.9	6.0 (MeOH)	99.4 Rose Bengal	[107]
Kevlar	NIPS	52	7.6 (MeOH)	95.4 Rose Bengal	[108]
PI/PEI	NIPS	91.2	28.8 (Hexane)	99.2 L-α-lecithin	[109]
TAPA-30-120	Crosslink	22.9	1.2 (IPA)	99.2 Rose Bengal	[62]
PAR@mBHPF0.2	IP	61.9	14.5 (MeOH)	98 700 Da	[110]
COP-30	IP	89	10.0 (Toluene)	91 Rhodanile	[111]
CBPPO20	Crosslink	63.1	9.1 (EtOH)	99.9 Rose Bengal	[112]
PFPE/PI	Coating	124	0.52 (IPA)	92.7 Orange II	[113]
PANI-0.2)d/HPAN	Self-polymerization	45.5	14.9 (EtOH)	98.1 Rose Bengal	[114]
PBSA-15	Crosslink	92.8	4.7 (DMAc)	90 844 Da	[115]
TFC-ZIF-8	IP	78	8.5 (MeOH)	95.2 Sunset Yellow	[116]
APN-2.5@KANF	NIPS	68.2	6.5 (EtOH)	98.8 Rose Bengal	[117]
Hydrated ZIF-8/WS2	Vacuum filtration	60	25 (IPA)	87 Rose Bengal	[118]
PA/ZIF-8_1L	IP	59	8.7 (MeOH)	90 Sunset Yellow	[119]
TFN-2	IP	31	3.3 (EtOH)	97 Rose Bengal	[120]
(PA-TTSBI/PI)xa	IP	58.5	5.9 (EtOH)	99 Rhodamine B	[121]
$PEG400/cPI_{1:2,\ 50\ W}$	Plasma	33.2	13.8 (EtOH)	83.6 Rose Bengal	[122]
S-PANI PAMPSA	NIPS	12	6.3 (THF)	90 645 Da	[123]
Noria + TPC	IP	61.5	18 (MeOH)	≈98 Rose Bengal	[124]
GM-10	Vacuum filtration	78	15.6 (EtOH)	85.6 Rose Bengal	[70]
(PEI/SWCNT)8-GA	LBL assembly	64.4	2.2 (EtOH)	99.2 Rose Bengal	[34]
(PEI/PSS-CNT)10	LBL assembly	54.7	2.5 (EtOH)	98 Rose Bengal	[125]
FPN-TFC	IP	38.8	1.1 (EtOH)	99.5 Rose Bengal	[126]
sPPSU-C-ECH	Crosslink	56.6	11.9 (EtOH)	93 645 Da	[127]
DTAC-TFC	IP	82	4.8 (MeOH)	99.0 Acid Red 27	[128]
PANI-PAMPSA	NIPS	62.8	0.55 (MeOH)	90 400 Da	[129]
CTP/PAN	IP	75.6	2.6 (MeOH)	97 Reactive Black 5	[130]
BPAF-TMC/PAN	IP	116.3	124.1 (MeOH)	99.2 CBBR	[131]
AOPIM-1	IP	62	15.5 (EtOH)	90 800 Da	[132]
PA/cGO/Cross-linked PI	IP	55.7	4.1 (EtOH)	99.7 Rose Bengal	[67]
B-BOP	Solvothermal	75.3	7.2 (Acetone)	100 Rose Bengal	[133]

industry, bringing significant economic and environmental benefits to the industry.

5.1.2. Desulfurization of gasoline

To promote "green environmental" initiatives and reduce emissions, there has been a gradual tightening of the restrictions on sulfur levels permitted in gasoline. OSN technology holds promising potential as a solution for reducing sulfur content in gasoline. Various types of membranes, including polyimide film, polyurea-urethane, and polydioxanone, have been tested and found to be suitable options for implementing this process.

5.1.3. Deacidification of oil

To remove impurities such as organic acids that can cause corrosion issues in crude oil, polar solvents were typically used for extraction, with subsequent recovery through distillation. OSN has the potential to revolutionize the deacidification of non-edible and waste oils by offering versatility and the capability to process oils with diverse compositions, making it a promising and valuable technology for the sustainable utilization of oil resources [2]. BP has patented an alternative process to distillation, which was a thermal separation process with high energy costs. In this alternative process, the use of OSN enables the recovery of the extraction solvent in the permeate, while keeping organic acids and neutralization salts in the recirculating fluid [135].

5.2. Chemical engineering

Nair et al. evaluated and assessed the efficiency of the palladium Heck catalyst in a cyclic batch recycling procedure that utilized OSN membranes [136]. According to the study conducted by Franke et al. satisfactory results were observed with PDMS in terms of its performance in paraffin and olefins. Based on these findings, Schoeps et al. found high catalyst rejection of bulk Grubbs complexes by PDMS membranes in olefin methanation reactions, suggesting that PDMS membranes have a wide range of applications in catalyst recovery [13] (see Fig. 16).

There were three kinds of process flow for OSN catalyst recovery: intermittent, semi-continuous, and continuous. For large-scale production, both semi-continuous and continuous processes are a proper choice due to their increased financial advantages and operational effectiveness [137]. Through single-stage membrane separation as illustrated in Fig. 17, Priske et al. employed an OSN continuous process to achieve a 99 % rejection rate and recover the Rh catalyst in the hydroformylation of higher olefins [136]. Schmidt et al. highlighted the potential for significant cost savings in homogeneous catalysis through the application of OSN, estimating potential annual savings in the millions of Euros. This technology has already been successfully implemented on an industrial scale, such as at Evonik Industries AG, for the rejection of homogeneous catalysts [138].

5.3. Solvent recovery

In the organic solvent recovery process known as OSN, the power usage per unit volume of organic solvents was found to be approximately 1/25th of that in classical separation processes, indicating significant energy savings [139]. The separation and purification of organic solvents using OSN was recognized as a highly effective, eco-friendly, and energy-efficient method [140]. Furthermore, the OSN technique allowed for the simultaneous concentration of small active molecules, leading to a reduction in the loss of expensive active components [141].

OSN, a technique employed for organic solvent recovery, demonstrates noteworthy energy efficiencies. Compared to classical separation processes, OSN's power consumption per unit volume of organic solvents is approximately only 1/25th, pointing to substantial energy savings [139]. Not only is the OSN method considered eco-friendly and energy-efficient for separating and purifying organic solvents [140], but it also permits the concurrent concentration of small active molecules. This results in minimizing the loss of costly active components [141].

5.3.1. Two-stage OSN process

The two-stage OSN process described by Schnitzer et al. focuses on the gentle separation of low molecular impurities. Due to the

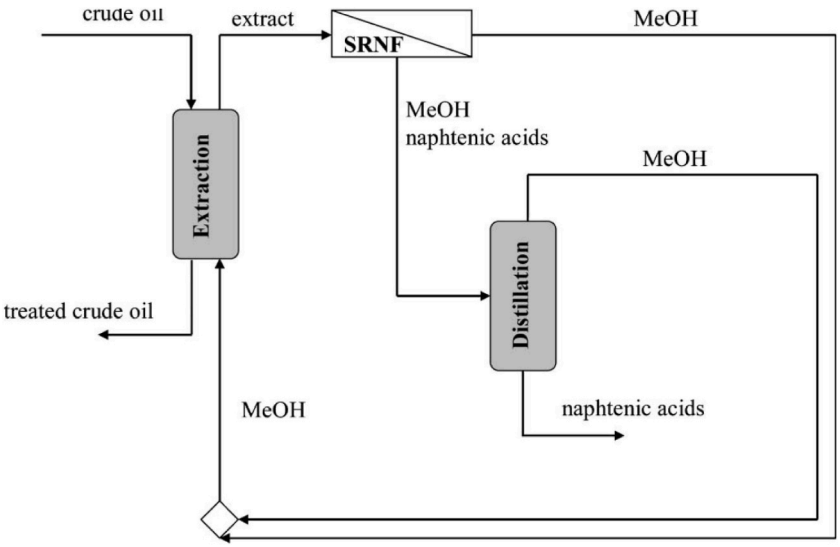

Fig. 16. Schematic diagram of crude oil desalting process [135].

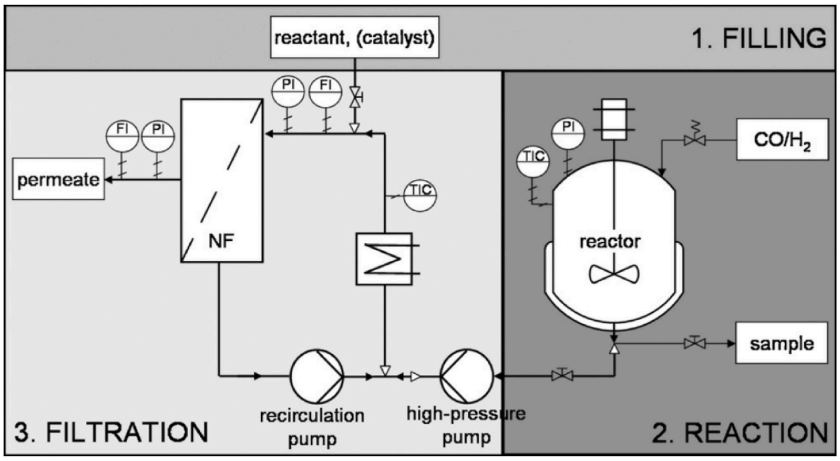

Fig. 17. Diagram depicting the experimental setup for hydroformylation [136].

product's limited thermal resistance and the increasingly stringent purity requirements, the separation method previously employed involved evaporation. However, to meet these requirements and address the limitations of thermal resistance, OSN was introduced into the downstream process. In the first stage of the process, a larger-pore membrane was used to remove larger molecular impurities or unwanted components from the mixture. After the first stage, the mixture was passed through a second, smaller-pore membrane. This membrane selectively blocks the passage of lower molecular weight impurities, allowing higher molecular weight components to pass through. The second OSN step was crucial for achieving economic viability; without it, cost-effectiveness goals would not be met [142]. The two-stage OSN process offers the advantage of a gentle separation technique, operating at lower pressures and temperatures, which was particularly advantageous for temperature-sensitive components or delicate molecules.

5.3.2. Methanol recovery

Bournay et al.'s patent introduces ethanol-selective membranes for separation in a multi-step reaction process. The key points of this patent include.

- Use of ethanol-selective membranes, specifically the Starmem 120 membrane
- Operating conditions: 50 °C temperature and 60 bar pressure
- Separation results in a retentate with 15 wt% lower methanol content
- Enriched methanol permeate was recycled back into the reactor for sustainability
- Significant reduction in resource consumption compared to classical separation method: half of decrease in high-pressure vapor、over half reduction of cooling water、complete elimination of low-pressure vapor.

This demonstrates the potential of membrane separation to improve efficiency and reduce the bad impacts on the environment.

5.4. Pharmaceuticals

5.4.1. API (active pharmaceutical Ingredient)Concentration and purification

Organic solvents contribute to 56 % of API materials and 80 % of pharmaceutical waste, emphasizing the need for their reduction to enhance environmental sustainability [143]. OSN can be used to concentrate many bioactive ingredients and API from solutions containing organic or aqueous solvents. The utilization of OSN offers advantages such as minimized solvent waste, enhanced cost-efficiency, and lowered energy consumption in the intermediate stages or subsequent processing of medication synthesis. By employing OSN, the concentration process becomes more efficient, resulting in optimized resource utilization and reduced environmental impact in medication manufacturing. Rong et al. developed a highly efficient hollow fiber membrane using crosslinked PI and hexaimide, capable of concentrating levofloxacin from 500 ppm to 20 000 ppm with a retention rate exceeding 95 % [140]. Guowu et al. prepared a novel PMIA/Co-PIP/PA membrane and demonstrated excellent performance including a high ethanol permeance rate, high rejection rate for organic solutes with molecular weights above 697 Da, and sustained stability in erythromycin/methanol separation [144].

5.4.2. Chiral separations

OSN has been utilized for chiral separations as well. One method called OSN-combined enantioselective inclusion-complexation, involves the utilization of pristine chiral carriers. This approach operates at high concentrations and ambient temperature as seen in Fig. 18 [135].

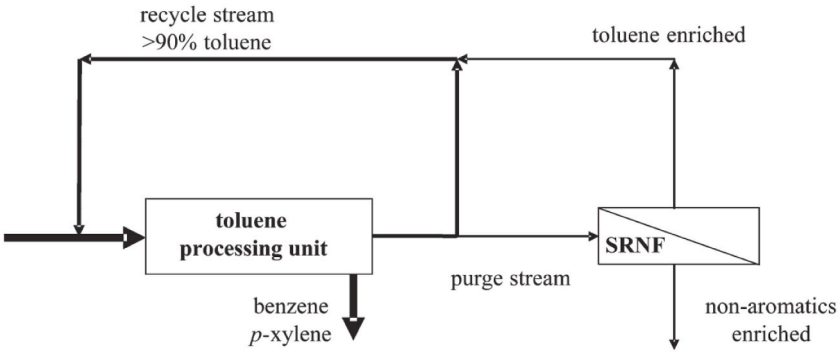

Fig. 18. Schematic diagram of the use of OSN in a toluene purification process [135].

5.5. Food industry

5.5.1. Edible oil process

The primary constituent of crude vegetable oil was triglycerides (TGs), which may also contain minor amounts of phospholipids and free fatty acids (FFAs). These impurities, particularly the FFAs, can have a negative impact on the quality of the oil. The primary constituent of crude vegetable oil was triglycerides (TGs), which may also contain minor amounts of phospholipids and free fatty acids (FFAs) [47]. In the study by Darvishmanesh et al. a commercial Starmem 122 membrane was used to recover ethanol from an edible oil solution, resulting in an ethanol flux of 9 kg m^{-2} h^{-1}·MPa^{-1} and an oil retention rate of 96.0 % [145]. Shi et al. proposed a two-step membrane process for efficient solvent recovery from oil compounds using business OSN membranes as illustrated in Fig. 19 to separate triglyceride solubilization from free fatty acids while achieving solvent recovery [146].

5.5.2. Extract biologically active ingredients

Monte et al. utilized OSN (Organic Solvent Nanofiltration) membranes, specifically DuraMem 300 and DuraMem500, to separate thermosensitive biologically active ingredients such as carotene, vitamins, carotenoids, and natural vegetable oil. They focused on separating carotenoids from free fatty acids (FFAs) and glycerol from proteins and carbohydrates. OSN holds significant prospects in the extraction of bioactive components because of its mild operating conditions and minimal damage to natural active substances.

5.6. Organic dye wastewater treatment

The high concentration of dye wastewater has resulted in significant environmental contamination and directly affected the sustainable growth of the dye industry. Due to the rising demands of the government and society regarding environmental protection, it has become imperative to develop efficient methods and processes for the treatment of dye wastewater. PPTA/PPy OSN membranes still exhibit excellent filtration performance under harsh conditions such as high temperatures and organic solvents [147]. Mahdavi et al. prepared a novel TFC membrane using a high-density polyethylene membrane scaffold, which showed high rejection of dyes [148]. Baowei et al. incorporated functionalized MoS2 nanosheets into a thin film nanocomposite of extremely smooth and incredibly thin polyamide, resulting in a 99.1 % rejection rate for the dye Rhodamine B [149].

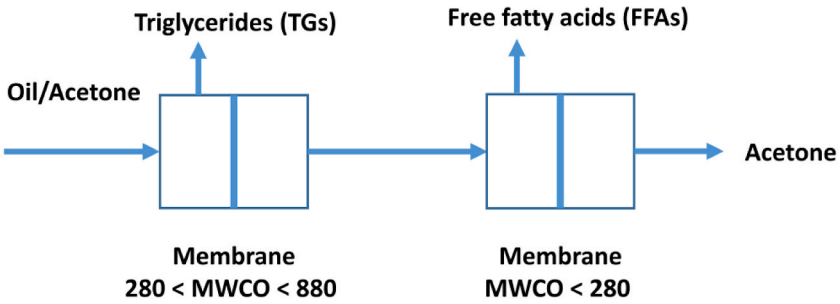

Fig. 19. Schematic illustration showcasing the principle behind the two-stage separation and the subsequent recuperation of acetone with OSN membranes [146].

6. Industrialization

6.1. Commercial OSN membranes

According to the type of material produced, commercial OSN membranes were typically classified into polymer and ceramic membranes. The most extensively used commercial OSN membranes worldwide were the SelRO® series from Koch Separation Solutions (KSS), the oNF-1, oNF-2, and oNF-3 from BORSIG Membrane Technology GmbH, and the DuraMem® and PuraMem® from Evonik Industries. Evonik's DuraMem® series was prepared by crosslinked P84 polyimide and was suitable for polar solvent environments. The PuraMem® series was formed by silicone chemistry and was suitable for apolar solvent and high boiling point solvent systems. Membranes from BORSIG constructed with silicone rubber (PDMS) showed stability in aromatics, alkanes, alcohols, ethers, and ketones. Currently, there are no commercially available hydrophobic ceramic nanofiltration membranes for OSN, although the Vankelekoms group has reported on HITK-T1 using IKTS.

6.2. Scale production

DuraMem® and PuraMem® series, which were designed specifically for chemical resistance were currently leaders of the OSN market. DuraMem® can be used in most polar solvents and polar non-protonic solvents (Acetone, THF, DMF, IPA, ACN, MEK, Ethyl acetate, etc.) with good long-term stability. The PuraMem® was appropriate for apolar hydrocarbon-type solvents (Toluene, Heptane, Hexane, Methylethylketone, Methyl-isobutyl ketone, Ethyl acetate, etc.) and has good stability in practical applications. Table 2 showed the basic properties of the two membranes mentioned above.

A patented membrane created by KSS with highly cross-linked polymer chemistry was a feature of SelRO® spiral wrap elements. With concentrations of up to 20 % for sodium and potassium hydroxide and up to 35 % for sulfuric, nitric, hydrochloric, hydrofluoric, and phosphoric acids, or acid blends, SelRO® membranes can process acids and bases at temperatures as high as 160 °F (70 °C). The membranes also have a very long service life and exceptional long-term stability.

BORSIG OSN Membranes oNF-1, oNF-2, and oNF-3 were renowned for their exceptional performance and have great stability in a variety of organic solvents. These membranes were long-lasting and had strong chemical resistance to solvents such as alkanes, aromatics, alcohols, ethers, ketones, and esters, as well as mechanical stability up to 40 bar and 80 °C. Of these, oNF-2 was the most selective membrane and was typically employed in fine and specialty chemistry, while oNF-3 exhibits unusually high flux in non-polar solvents and was particularly suited for bulk applications.

7. Conclusion

In this work, we recapped the history, theory, mechanism, and evaluation of OSN at first. Generally, in the past decade, various researchers paid attention to developing novel materials applied for OSN and how to modify the membrane to obtain better filtration performance. Also, the relationship between solute, solvent, and membrane was extensively explored. However, there was little research on whether OSN films tend to be hydrophilic or hydrophobic. We introduced crucial studies on both hydrophilic and hydrophobic OSN membranes classified by different types of membranes. Hydrophilic surface benefited the transmembrane transport of polar solvents while hydrophobic surface facilitated the permeation of non-polar solvents. Therefore, in the test of polar solvents, OSN membranes tended to pursue a more hydrophilic surface, while in the test of non-polar solvents, OSN membrane tended to prefer a more hydrophobic surface. We listed a large number of hydrophilic and hydrophobic OSN membranes and filtration performance for comparison according to different solvents. Finally, in view of OSN engineering application, we summarized some industrial cases of hydrophilic OSN membranes and hydrophobic OSN membranes including solvent recovery, solvent change, pharmaceuticals, food industries, and so on. The research on the hydrophilicity of the membrane surface gave a new angle for the future study of OSN membranes, which was likely to break through the current filtration performance in terms of permeation and selectivity to meet the requirements of future OSN applications.

Additional information

No additional information is available for this paper.

Table 2
The performance data of Puramem® and Duramem®.

Details	Puramem®	Duramem®
Types	flat sheets and spiral wound membrane modules	flat sheets and spiral wound membrane modules
Molecular weight cutoff range	280–600 Da	150–900 Da
Maximum temperature	50 °C	50 °C
Maximum operating pressure	from 20 to 60 bar	from 20 to 60 bar
Application	toluene, heptane, hexane, methylethylketone, methyl-isobutyl ketone, and more	Acetone, Tetrahydrofuran, Methanol, Ethanol, Dimethylformamide and more

CRediT authorship contribution statement

Yi-Hao Tong: Writing - original draft, Writing - review & editing, Supervision, Methodology, Conceptualization. **Li-Han Luo:** Writing - original draft, Investigation, Data curation, Conceptualization. **Rui Jia:** Writing - original draft, Investigation. **Rui Han:** Writing - original draft, Investigation. **Sun-Jie Xu:** Writing - original draft, Methodology, Investigation, Funding acquisition. **Zhen-Liang Xu:** Investigation.

Declaration of competing interest

The authors declare that they have no known competing financial interests or personal relationships that could have appeared to influence the work reported in this paper.

Acknowledgements

The authors gratefully acknowledge the financial support received from the Project funded by State Key R&D Program of China (2021YFB3801101 and 2021YFB3801103) and National Natural Science Foundation of China (22208101) as well as the research funding provided by the Fundamental Research Funds for the Central Universities (JKA01231522).

References

[1] P. Marchetti, M.F. Jimenez Solomon, G. Szekely, A.G. Livingston, Molecular separation with organic solvent nanofiltration: a critical review, Chem. Rev. 114 (21) (2014) 10735–10806, https://doi.org/10.1021/cr500006j.
[2] P.K. Kathrin Werth, Mirko Skiborowski ⇑, The Potential of Organic Solvent Nanofiltration Processes for Oleochemical Industry, Separation and Purification Technology, 2017, https://doi.org/10.1016/j.seppur.2017.03.050.
[3] J.H. Aburabie, T. Puspasari, K.-V. Peinemann, Alginate-based membranes: paving the way for green organic solvent nanofiltration, J. Membr. Sci. 596 (2020), https://doi.org/10.1016/j.memsci.2019.117615.
[4] D. Chen, S. Yu, H. Zhang, X. Li, Solvent resistant nanofiltration membrane based on polybenzimidazole, Separ. Purif. Technol. 142 (2015) 299–306, https://doi.org/10.1016/j.seppur.2015.01.011.
[5] L. Paseta, J.M. Luque-Alled, M. Malankowska, M. Navarro, P. Gorgojo, J. Coronas, C. Téllez, Functionalized graphene-based polyamide thin film nanocomposite membranes for organic solvent nanofiltration, Separ. Purif. Technol. 247 (2020), https://doi.org/10.1016/j.seppur.2020.116995.
[6] S. Kim, K.H. Chu, Y.A.J. Al-Hamadani, C.M. Park, M. Jang, D.-H. Kim, M. Yu, J. Heo, Y. Yoon, Removal of contaminants of emerging concern by membranes in water and wastewater: a review, Chem. Eng. J. 335 (2018) 896–914, https://doi.org/10.1016/j.cej.2017.11.044.
[7] M.-L. Liu, J.-L. Guo, S. Japip, T.-Z. Jia, D.-D. Shao, S. Zhang, W.-J. Li, J. Wang, X.-L. Cao, S.-P. Sun, One-step enhancement of solvent transport, stability and photocatalytic properties of graphene oxide/polyimide membranes with multifunctional cross-linkers, J. Mater. Chem. A 7 (7) (2019) 3170–3178, https://doi.org/10.1039/c8ta11372f.
[8] Q. Liu, S.J.D. Smith, K. Konstas, D. Ng, K. Zhang, M.R. Hill, Z. Xie, Construction of ultrathin PTMSP/Porous nanoadditives membranes for highly efficient organic solvent nanofiltration (OSN), J. Membr. Sci. 620 (2021), https://doi.org/10.1016/j.memsci.2020.118911.
[9] T. Huang, B.A. Moosa, P. Hoang, J. Liu, S. Chisca, G. Zhang, M. AlYami, N.M. Khashab, S.P. Nunes, Molecularly-porous ultrathin membranes for highly selective organic solvent nanofiltration, Nat. Commun. 11 (1) (2020), https://doi.org/10.1038/s41467-020-19404-6.
[10] G.M. Shi, Y. Feng, B. Li, H.M. Tham, J.-Y. Lai, T.-S. Chung, Recent progress of organic solvent nanofiltration membranes, Prog. Polym. Sci. 123 (2021), https://doi.org/10.1016/j.progpolymsci.2021.101470.
[11] C.S. Sourirajan, Separation of hydrocarbon liquids by flow under pressure through porous MEMBRANESCR. S. Sourirajan, Nature 203 (1964) 1348–1349.
[12] S. Ali, I.A. Shah, I. Ihsanullah, X. Feng, Nanocomposite membranes for organic solvent nanofiltration: recent advances, challenges, and prospects, Chemosphere 308 (Pt 2) (2022) 136329, https://doi.org/10.1016/j.chemosphere.2022.136329.
[13] M. Priske, M. Lazar, C. Schnitzer, G. Baumgarten, Recent applications of organic solvent nanofiltration, Chem. Ing. Tech. 88 (1–2) (2016) 39–49, https://doi.org/10.1002/cite.201500084.
[14] Y.H. See Toh, F.W. Lim, A.G. Livingston, Polymeric membranes for nanofiltration in polar aprotic solvents, J. Membr. Sci. 301 (1–2) (2007) 3–10, https://doi.org/10.1016/j.memsci.2007.06.034.
[15] M.F. Jimenez Solomon, Y. Bhole, A.G. Livingston, High flux membranes for organic solvent nanofiltration (OSN)—interfacial polymerization with solvent activation, J. Membr. Sci. 423–424 (2012) 371–382, https://doi.org/10.1016/j.memsci.2012.08.030.
[16] H.K. Lonsdale, U. Merten, R.L. Riley, Transport properties of cellulose acetate osmotic membranes, J. Appl. Polym. Sci. 9 (4) (1965) 1341–1362, https://doi.org/10.1002/app.1965.070090413.
[17] J.G. Wijmans, R.W. Baker, The solution-diffusion model: a review, J. Membr. Sci. 107 (1) (1995) 1–21, https://doi.org/10.1016/0376-7388(95)00102-I.
[18] W.R. Bowen, J.S. Welfoot, Modelling of membrane nanofiltration—pore size distribution effects, Chem. Eng. Sci. 57 (8) (2002) 1393–1407, https://doi.org/10.1016/S0009-2509(01)00412-2.
[19] A.E. Yaroshchuk, Solution-diffusion-imperfection model revised, J. Membr. Sci. 101 (1) (1995) 83–87, https://doi.org/10.1016/0376-7388(94)00277-6.
[20] O. Kedem, A. Katchalsky, Thermodynamic analysis of the permeability of biological membranes to non-electrolytes, Biochim. Biophys. Acta 27 (1958) 229–246, https://doi.org/10.1016/0006-3002(58)90330-5.
[21] K.S. Spiegler, O. Kedem, Thermodynamics of hyperfiltration (reverse osmosis): criteria for efficient membranes, Desalination 1 (4) (1966) 311–326, https://doi.org/10.1016/S0011-9164(00)80018-1.
[22] P. Vandezande, L.E.M. Gevers, I.F.J. Vankelecom, Solvent resistant nanofiltration: separating on a molecular level, Chem. Soc. Rev. 37 (2) (2008) 365–405, https://doi.org/10.1039/B610848M.
[23] J. Labanda, J. Sabaté, J. Llorens, Permeation of organic solutes in water–ethanol mixtures with nanofiltration membranes, Desalination 315 (2013) 83–90, https://doi.org/10.1016/j.desal.2012.10.007.
[24] P.C. Meares, J B, J. Webster, Diffusion processes, in: J.N. Sherwood, A.V. Chadwick, W.M. Muir, F.L. Swinton (Eds.), DIFFUSION PROCESSES. VOLUME I, Proceedings of the Thomas Graham Memorial Symposium, Strathclyde, Scotland, September 22–24, 1969, 1971.
[25] H. Yasuda, A. Peterlin, Diffusive and bulk flow transport in polymers, J. Appl. Polym. Sci. 17 (2) (1973) 433–442, https://doi.org/10.1002/app.1973.070170209.
[26] E.A. Mason, H.K. Lonsdale, Statistical-mechanical theory of membrane transport, J. Membr. Sci. 51 (1) (1990) 1–81, https://doi.org/10.1016/S0376-7388(00)80894-7.
[27] P.D.P. Atkins, J. Atkins', Physical chemistry, in: Atkins' Physical Chemistry, eighth ed., Oxford University Press, New York, 2006.
[28] D.R. Paul, Reformulation of the solution-diffusion theory of reverse osmosis, J. Membr. Sci. 241 (2) (2004) 371–386, https://doi.org/10.1016/j.memsci.2004.05.026.

[29] H.K. Lonsdale, U. Merten, M. Tagami, Phenol transport in cellulose acetate membranes, J. Appl. Polym. Sci. 11 (9) (1967) 1807–1820, https://doi.org/10.1002/app.1967.070110917.

[30] S.-I. Nakao, S. Kimura, Models of membrane transport phenomena and their applications for ultrafiltration data, J. Chem. Eng. Jpn. 15 (3) (1982) 200–205, https://doi.org/10.1252/jcej.15.200.

[31] A. Verniory, R. Du Bois, P. Decoodt, J.P. Gassee, P.P. Lambert, Measurement of the permeability of biological membranes application to the glomerular wall, J. Gen. Physiol. 62 (4) (1973) 489–507, https://doi.org/10.1085/jgp.62.4.489%JJournalofGeneralPhysiology.

[32] P. Marchetti, M.F.J. Solomon, G. Szekely, A.G. Livingston, Molecular separation with organic solvent nanofiltration: a critical review, Chem. Rev. 114 (21) (2014) 10735–10806, https://doi.org/10.1021/cr500006j.

[33] A. Krupková, M. Müllerová, R. Petrickovic, T. Strašák, On the edge between organic solvent nanofiltration and ultrafiltration: characterization of regenerated cellulose membrane with aspect on dendrimer purification and recycling, Separ. Purif. Technol. 310 (2023) 123141, https://doi.org/10.1016/j.seppur.2023.123141.

[34] C. Wang, M.J. Park, R.R. Gonzales, S. Phuntsho, H. Matsuyama, E. Drioli, H.K. Shon, Novel organic solvent nanofiltration membrane based on inkjet printing-assisted layer-by-layer assembly, J. Membr. Sci. 655 (2022), https://doi.org/10.1016/j.memsci.2022.120582.

[35] E. Bormashenko, Progress in understanding wetting transitions on rough surfaces, Adv. Colloid Interface Sci. 222 (2015) 92–103, https://doi.org/10.1016/j.cis.2014.02.009.

[36] J.C. Fernandez-Toledano, T.D. Blake, P. Lambert, J. De Coninck, On the cohesion of fluids and their adhesion to solids: young's equation at the atomic scale, Adv. Colloid Interface Sci. 245 (2017) 102–107, https://doi.org/10.1016/j.cis.2017.03.006.

[37] A. Khandan, M. Abdellahi, N. Ozada, H. Ghayour, Study of the bioactivity, wettability and hardness behaviour of the bovine hydroxyapatite-diopside bio-nanocomposite coating, J. Taiwan Inst. Chem. Eng. 60 (2016) 538–546, https://doi.org/10.1016/j.jtice.2015.10.004.

[38] Y.C. Xu, X.Q. Cheng, J. Long, L. Shao, A novel monoamine modification strategy toward high-performance organic solvent nanofiltration (OSN) membrane for sustainable molecular separations, J. Membr. Sci. 497 (2016) 77–89, https://doi.org/10.1016/j.memsci.2015.09.029.

[39] Y. Xu, F. You, H. Sun, L. Shao, Realizing mussel-inspired polydopamine selective layer with strong solvent resistance in nanofiltration toward sustainable reclamation, ACS Sustain. Chem. Eng. 5 (6) (2017) 5520–5528, https://doi.org/10.1021/acssuschemeng.7b00871.

[40] D. Zhao, J.F. Kim, G. Ignacz, P. Pogany, Y.M. Lee, G. Szekely, Bio-inspired robust membranes nanoengineered from interpenetrating polymer networks of polybenzimidazole/polydopamine, ACS Nano 13 (1) (2019) 125–133, https://doi.org/10.1021/acsnano.8b04123.

[41] H. Zhang, X. Li, C. Zhao, T. Fu, Y. Shi, H. Na, Composite membranes based on highly sulfonated PEEK and PBI: morphology characteristics and performance, J. Membr. Sci. 308 (1–2) (2008) 66–74, https://doi.org/10.1016/j.memsci.2007.09.045.

[42] I.B. Valtcheva, P. Marchetti, A.G. Livingston, Cross linked polybenzimidazole membranes for organic solvent nanofiltration (OSN): analysis of crosslinking reaction mechanism and effects of reaction parameters, J. Membr. Sci. 493 (2015) 568–579, https://doi.org/10.1016/j.memsci.2015.06.056.

[43] A. Oxley, A.G. Livingston, Anti-fouling membranes for organic solvent nanofiltration (OSN) and organic solvent ultrafiltration (OSU): graft modified polybenzimidazole (PBI), J. Membr. Sci. 662 (2022) 120977, https://doi.org/10.1016/j.memsci.2022.120977.

[44] A. El-Gendi, E. Favre, D. Roizard, Asymmetric polyetherimide membranes (PEI) for nanofiltration treatment, Eur. Polym. J. 105 (2018) 204–216, https://doi.org/10.1016/j.eurpolymj.2018.06.001.

[45] A.V. Volkov, S.E. Tsarkov, A.B. Gilman, V. Khotimsky, V.I. Roldughin, V.V. Volkov, Surface modification of PTMSP membranes by plasma treatment: asymmetry of transport in organic solvent nanofiltration, Adv. Colloid Interface Sci. 222 (2015) 716–727, https://doi.org/10.1016/j.cis.2014.11.005.

[46] P. Jin, S. Yuan, G. Zhang, J. Zhu, J. Zheng, P. Luis, B. Van der Bruggen, Polyarylene thioether sulfone/sulfonated sulfone nanofiltration membrane with enhancement of rejection and permeability via molecular design, J. Membr. Sci. 608 (2020) 118241, https://doi.org/10.1016/j.memsci.2020.118241.

[47] U.G. Thummar, M. Saxena, S. Ray, P.S. Singh, Solvent-resistant polyvinyl alcohol nanofilm with nanopores for high-flux degumming, J. Membr. Sci. 650 (2022), https://doi.org/10.1016/j.memsci.2022.120430.

[48] S. Foroutan, M. Hashemian, M. Khosravi, M.G. Nejad, A. Asefnejad, S. Saber-Samandari, A. Khandan, A porous sodium alginate-CaSiO3 polymer reinforced with graphene nanosheet: fabrication and optimality analysis, Fibers Polym. 22 (2) (2021) 540–549, https://doi.org/10.1007/s12221-021-0347-9.

[49] A. Raisi, A. Asefnejad, M. Shahali, Z. Sadat Kazerouni, A. Kolooshani, S. Saber-Samandari, B. Moghadas, A. Khandan, Preparation, characterization, and antibacterial studies of N, O-carboxymethyl chitosan as a wound dressing for bedsore application, Archives of Trauma Research 9 (4) (2020) 181–188, https://doi.org/10.4103/atr.atr_10_20.

[50] P. Jin, S. Yuan, G. Zhang, J. Zhu, J. Zheng, P. Luis, B. Van der Bruggen, Polyarylene thioether sulfone/sulfonated sulfone nanofiltration membrane with enhancement of rejection and permeability via molecular design, J. Membr. Sci. 608 (2020), https://doi.org/10.1016/j.memsci.2020.118241.

[51] N. Ranjbari, M. Razzaghi, R. Fernandez-Lafuente, F. Shojaei, M. Satari, A. Homaei, Improved features of a highly stable protease from Penaeus vannamei by immobilization on glutaraldehyde activated graphene oxide nanosheets, Int. J. Biol. Macromol. 130 (2019) 564–572, https://doi.org/10.1016/j.ijbiomac.2019.02.163.

[52] M.M. Safaei, R. Abedinzadeh, A. Khandan, R. Barbaz-Isfahani, D. Toghraie, Synergistic effect of graphene nanosheets and copper oxide nanoparticles on mechanical and thermal properties of composites: experimental and simulation investigations, Mater. Sci. Eng., B 289 (2023) 116248, https://doi.org/10.1016/j.mseb.2022.116248.

[53] I. Soroko, A. Livingston, Impact of TiO2 nanoparticles on morphology and performance of crosslinked polyimide organic solvent nanofiltration (OSN) membranes, J. Membr. Sci. 343 (1–2) (2009) 189–198, https://doi.org/10.1016/j.memsci.2009.07.026.

[54] A. Dobrak, B. Verrecht, H. Van den Dungen, A. Buekenhoudt, I.F.J. Vankelecom, B. Van der Bruggen, Solvent flux behavior and rejection characteristics of hydrophilic and hydrophobic mesoporous and microporous TiO2 and ZrO2 membranes, J. Membr. Sci. 346 (2) (2010) 344–352, https://doi.org/10.1016/j.memsci.2009.09.059.

[55] A. Homaei, Enzyme immobilization and its application in the food industry, Advances in Food Biotechnology (2015) 145–164, https://doi.org/10.1002/9781118864463.ch09.

[56] M. Razzaghi, A. Homaei, F. Vianello, T. Azad, T. Sharma, A.K. Nadda, R. Stevanato, M. Bilal, H.M.N. Iqbal, Industrial applications of immobilized nano-biocatalysts, Bioproc. Biosyst. Eng. 45 (2) (2022) 237–256, https://doi.org/10.1007/s00449-021-02647-y.

[57] A. Homaei, Immobilization of Penaeus merguiensis alkaline phosphatase on gold nanorods for heavy metal detection, Ecotoxicol. Environ. Saf. 136 (2017) 1–7, https://doi.org/10.1016/j.ecoenv.2016.10.023.

[58] F. Zeinali, A. Homaei, E. Kamrani, S. Patel, Use of Cu/Zn-superoxide dismutase tool for biomonitoring marine environment pollution in the Persian Gulf and the Gulf of Oman, Ecotoxicol. Environ. Saf. 151 (2018) 236–241, https://doi.org/10.1016/j.ecoenv.2018.01.029.

[59] M.H.D.A. Farahani, D. Hua, T.-S. Chung, Cross-linked mixed matrix membranes (MMMs) consisting of amine-functionalized multi-walled carbon nanotubes and P84 polyimide for organic solvent nanofiltration (OSN) with enhanced flux, J. Membr. Sci. 548 (2018) 319–331, https://doi.org/10.1016/j.memsci.2017.11.037.

[60] Z. Si, Z. Wang, D. Cai, G. Li, S. Li, P. Qin, A high-permeance organic solvent nanofiltration membrane via covalently bonding mesoporous MCM-41 with polyimide, Separ. Purif. Technol. 241 (2020), https://doi.org/10.1016/j.seppur.2020.116545.

[61] Y. Shen, A. Yao, J. Li, D. Hua, K.B. Tan, G. Zhan, X. Rao, Dispersive two-dimensional MXene via potassium fulvic acid for mixed matrix membranes with enhanced organic solvent nanofiltration performance, J. Membr. Sci. 666 (2023) 121168, https://doi.org/10.1016/j.memsci.2022.121168.

[62] Z.F. Gao, Y. Feng, D. Ma, T.-S. Chung, Vapor-phase crosslinked mixed matrix membranes with UiO-66-NH2 for organic solvent nanofiltration, J. Membr. Sci. 574 (2019) 124–135, https://doi.org/10.1016/j.memsci.2018.12.064.

[63] Y. Shen, A. Yao, J. Li, D. Hua, K.B. Tan, G. Zhan, X. Rao, Dispersive two-dimensional MXene via potassium fulvic acid for mixed matrix membranes with enhanced organic solvent nanofiltration performance, J. Membr. Sci. 666 (2023), https://doi.org/10.1016/j.memsci.2022.121168.

[64] A.W. Mohammad, Y.H. Teow, W.L. Ang, Y.T. Chung, D.L. Oatley-Radcliffe, N. Hilal, Nanofiltration membranes review: recent advances and future prospects, Desalination 356 (2015) 226–254, https://doi.org/10.1016/j.desal.2014.10.043.

[65] G.M. Shi, Y. Feng, B. Li, H.M. Tham, J.-Y. Lai, T.-S. Chung, Recent progress of organic solvent nanofiltration membranes, Prog. Polym. Sci. 123 (2021) 101470, https://doi.org/10.1016/j.progpolymsci.2021.101470.

[66] S. Sorribas, P. Gorgojo, C. Tellez, J. Coronas, A.G. Livingston, High flux thin film nanocomposite membranes based on metal-organic frameworks for organic solvent nanofiltration, J. Am. Chem. Soc. 135 (40) (2013) 15201–15208, https://doi.org/10.1021/ja407665w.

[67] Y. Li, C. Li, S. Li, B. Su, L. Han, B. Mandal, Graphene oxide (GO)-interlayered thin-film nanocomposite (TFN) membranes with high solvent resistance for organic solvent nanofiltration (OSN), J. Mater. Chem. A 7 (21) (2019) 13315–13330, https://doi.org/10.1039/c9ta01915d.

[68] J. Liu, D. Hua, Y. Zhang, S. Japip, T.-S. Chung, Precise molecular sieving architectures with Janus pathways for both polar and nonpolar molecules, Adv. Mater. 30 (11) (2018), https://doi.org/10.1002/adma.201705933.

[69] M.F. Jimenez-Solomon, Q. Song, K.E. Jelfs, M. Munoz-Ibanez, A.G. Livingston, Polymer nanofilms with enhanced microporosity by interfacial polymerization, Nat. Mater. 15 (7) (2016) 760, https://doi.org/10.1038/nmat4638.

[70] A. Wang, W. Chen, H. Xu, Z. Xie, X. Zheng, M. Liu, Y. Wang, N. Geng, X. Mu, M. Ding, Heterostructured MoS2 quantum dot/GO lamellar membrane with improved transport efficiency for organic solvents inspired by the Namib Desert beetle, J. Membr. Sci. 650 (2022), https://doi.org/10.1016/j.memsci.2022.120402.

[71] Q. Yang, Y. Su, C. Chi, C.T. Cherian, K. Huang, V.G. Kravets, F.C. Wang, J.C. Zhang, A. Pratt, A.N. Grigorenko, F. Guinea, A.K. Geim, R.R. Nair, Ultrathin graphene-based membrane with precise molecular sieving and ultrafast solvent permeation, Nat. Mater. 16 (12) (2017) 1198, https://doi.org/10.1038/nmat5025.

[72] L. Huang, J. Chen, T. Gao, M. Zhang, Y. Li, L. Dai, L. Qu, G. Shi, Reduced graphene oxide membranes for ultrafast organic solvent nanofiltration, Adv. Mater. 28 (39) (2016) 8669–8674, https://doi.org/10.1002/adma.201601606.

[73] H. Guo, S. Yu, T. Liu, Q.-F. An, X. Ren, Z. Qin, Y. Liang, Counterion-switched reversibly hydrophilic and hydrophobic TiO2-incorporated layer-by-layer self-assembled membrane for nanofiltration, Macromol. Mater. Eng. 304 (12) (2019), https://doi.org/10.1002/mame.201900481.

[74] M. Mertens, C. Van Goethem, M. Thijs, G. Koeckelberghs, I.F.J. Vankelecom, Crosslinked PVDF-membranes for solvent resistant nanofiltration, J. Membr. Sci. 566 (2018) 223–230, https://doi.org/10.1016/j.memsci.2018.08.051.

[75] C. Pagliero, N.A. Ochoa, P. Martino, J. Marchese, Separation of sunflower oil from hexane by use of composite polymeric membranes, J. Am. Oil Chem. Soc. 88 (11) (2011) 1813–1819, https://doi.org/10.1007/s11746-011-1839-3.

[76] L.R. Firman, N.A. Ochoa, J. Marchese, C. Pagliero, Designing of spiral wound nanofiltration multistage process for oil concentration and solvent recovery from soybean oil/n-hexane miscella, Chem. Eng. Res. Des. 164 (2020) 46–58, https://doi.org/10.1016/j.cherd.2020.09.015.

[77] C. Li, J. Li, W.-H. Zhang, N. Wang, S. Ji, Q.-F. An, Enhanced permeance for PDMS organic solvent nanofiltration membranes using modified mesoporous silica nanoparticles, J. Membr. Sci. 612 (2020), https://doi.org/10.1016/j.memsci.2020.118257.

[78] J. Ji, S. Mazinani, E. Ahmed, Y.M. John Chew, D. Mattia, Hydrophobic poly(vinylidene fluoride)/siloxene nanofiltration membranes, J. Membr. Sci. 635 (2021) 119447, https://doi.org/10.1016/j.memsci.2021.119447.

[79] S. Basu, M. Maes, A. Cano-Odena, L. Alaerts, D.E. De Vos, I.F.J. Vankelecom, Solvent resistant nanofiltration (SRNF) membranes based on metal-organic frameworks, J. Membr. Sci. 344 (1–2) (2009) 190–198, https://doi.org/10.1016/j.memsci.2009.07.051.

[80] A. Karimi, A. Khataee, M. Safarpour, V. Vatanpour, Development of mixed matrix ZIF-8/polyvinylidene fluoride membrane with improved performance in solvent resistant nanofiltration, Separ. Purif. Technol. 237 (2020), https://doi.org/10.1016/j.seppur.2019.116358.

[81] M.F. Jimenez Solomon, Y. Bhole, A.G. Livingston, High flux hydrophobic membranes for organic solvent nanofiltration (OSN)—interfacial polymerization, surface modification and solvent activation, J. Membr. Sci. 434 (2013) 193–203, https://doi.org/10.1016/j.memsci.2013.01.055.

[82] M.F. Jimenez-Solomon, P. Gorgojo, M. Munoz-Ibanez, A.G. Livingston, Beneath the surface: influence of supports on thin film composite membranes by interfacial polymerization for organic solvent nanofiltration, J. Membr. Sci. 448 (2013) 102–113, https://doi.org/10.1016/j.memsci.2013.06.030.

[83] S.I. Gnani Peer Mohamed, S. Nejati, M. Bavarian, All-polymeric thin-film nanocomposite membrane for organic solvent nanofiltration, ACS Appl. Polym. Mater. 3 (12) (2021) 6040–6044, https://doi.org/10.1021/acsapm.1c01291.

[84] S. Li, R. Dong, V.-E. Musteata, J. Kim, N.D. Rangnekar, J.R. Johnson, B.D. Marshall, S. Chisca, J. Xu, S. Hoy, B.A. McCool, S.P. Nunes, Z. Jiang, A.G. Livingston, Hydrophobic polyamide nanofilms provide rapid transport for crude oil separation, Science 377 (6614) (2022) 1555, https://doi.org/10.1126/science.abq0598.

[85] J. Kujawa, S. Cerneaux, W. Kujawski, Investigation of the stability of metal oxide powders and ceramic membranes grafted by perfluoroalkylsilanes, Colloids Surf. A Physicochem. Eng. Asp. 443 (2014) 109–117, https://doi.org/10.1016/j.colsurfa.2013.10.059.

[86] H. Guo, Y. Ma, Z. Qin, Z. Gu, S. Cui, G. Zhang, One-step transformation from hierarchical-structured superhydrophilic NF membrane into superhydrophobic OSN membrane with improved antifouling effect, ACS Appl. Mater. Interfaces 8 (35) (2016) 23379–23388, https://doi.org/10.1021/acsami.6b07106.

[87] C. Li, W. Zhen, Preparation, performance and structure-properties relationship of polyphenylene sulfide/ATP-PS/co-deposition of tannic acid nanocomposites membrane, Polym. Bull. (2023), https://doi.org/10.1007/s00289-023-04748-y.

[88] J. Chau, K.K. Sirkar, K.J. Pennisi, G. Vaseghi, L. Derdour, B. Cohen, Novel perfluorinated nanofiltration membranes for isolation of pharmaceutical compounds, Separ. Purif. Technol. 258 (2021) 117944, https://doi.org/10.1016/j.seppur.2020.117944.

[89] C.R. Tanardi, A. Nijmeijer, L. Winnubst, Coupled-PDMS grafted mesoporous gamma-alumina membranes for solvent nanofiltration, Separ. Purif. Technol. 169 (2016) 223–229, https://doi.org/10.1016/j.seppur.2016.05.057.

[90] Y. Lu, Z. Qin, N. Wang, Q.-F. An, H. Guo, Counterion exchanged hydrophobic polyelectrolyte multilayer membrane for organic solvent nanofiltration, J. Membr. Sci. 620 (2021), https://doi.org/10.1016/j.memsci.2020.118827.

[91] A. Waheed, U. Baig, I.H. Aljundi, Fabrication of molecularly porous hyper-cross-linked thin film composite nanofiltration membrane using cyclic amine and linear cross-linker for highly selective organic solvent nanofiltration, COLLOID AND INTERFACE SCIENCE COMMUNICATIONS 45 (2021), https://doi.org/10.1016/j.colcom.2021.100530.

[92] X. He, H. Sin, B. Liang, Z.A. Ghazi, A.M. Khattak, N.A. Khan, H.R. Alanagh, L. Li, X. Lu, Z. Tang, Controlling the selectivity of conjugated microporous polymer membrane for efficient organic solvent nanofiltration, Adv. Funct. Mater. 29 (32) (2019), https://doi.org/10.1002/adfm.201900134.

[93] A. Zhou, M.M.A. Almijbilee, J. Zheng, L. Wang, A thin film composite membrane prepared from monomers of vanillin and trimesoyl chloride for organic solvent nanofiltration, Separ. Purif. Technol. 263 (2021), https://doi.org/10.1016/j.seppur.2021.118394.

[94] S.-J. Xu, L.-H. Luo, Y.-H. Tong, Q. Shen, Z.-L. Xu, Y.-Z. Wu, H. Yang, Organic solvent nanofiltration (OSN) membrane with polyamantadinamide active layer for reducing separation performance inconformity, Separ. Purif. Technol. 278 (2022), https://doi.org/10.1016/j.seppur.2021.119582.

[95] A. Waheed, U. Baig, Exploiting phase inversion for penta-amine impregnation of ultrafiltration support matrix for rapid fabrication of a hyper-cross-linked polyamide membrane for organic solvent nanofiltration, Process Saf. Environ. Protect. 169 (2023) 24–33, https://doi.org/10.1016/j.psep.2022.10.072.

[96] C. Li, S. Li, L. Tian, J. Zhang, B. Su, M.Z. Hu, Covalent organic frameworks (COFs)-incorporated thin film nanocomposite (TFN) membranes for high-flux organic solvent nanofiltration (OSN), J. Membr. Sci. 572 (2019) 520–531, https://doi.org/10.1016/j.memsci.2018.11.005.

[97] C. Han, H. Liu, Y. Wang, An ultrapermeable thin film composite membrane supported by “green” nanofibrous polyimide substrate for polar aprotic organic solvent recovery, J. Membr. Sci. 644 (2022) 120192, https://doi.org/10.1016/j.memsci.2021.120192.

[98] H. Li, L. Huang, X. Li, W. Huang, L. Li, W. Li, M. Cai, Z. Zhong, Calcium-alginate/HKUST-1 interlayer-assisted interfacial polymerization reaction enhances performance of solvent-resistant nanofiltration membranes, Separ. Purif. Technol. 309 (2023), https://doi.org/10.1016/j.seppur.2022.123031.

[99] Y. Liang, C. Li, S. Li, B. Su, M.Z. Hu, X. Gao, C. Gao, Graphene quantum dots (GQDs)-polyethyleneimine as interlayer for the fabrication of high performance organic solvent nanofiltration (OSN) membranes, Chem. Eng. J. 380 (2020), https://doi.org/10.1016/j.cej.2019.122462.

[100] X. Li, W. Cai, T. Wang, Z. Wu, J. Wang, X. He, J. Li, AF2400/PTFE composite membrane for hexane recovery during vegetable oil production, Separ. Purif. Technol. 181 (2017) 223–229, https://doi.org/10.1016/j.seppur.2017.02.051.

[101] V. Berned-Samatan, M. Piantek, J. Coronas, C. Tellez, Nanofiltration with polyamide thin film composite membrane with ZIF-93/SWCNT intermediate layers on polyimide support, Separ. Purif. Technol. 308 (2023), https://doi.org/10.1016/j.seppur.2022.122915.

[102] P. Li, H. Xie, Y. Bi, C. Miao, K. Chen, T. Xie, S. Zhao, H. Sun, X. Yang, Y. Hou, J. Niu, Preparation of high flux organic solvent nanofiltration membrane based on polyimide/Noria composite ultrafiltration membrane, Appl. Surf. Sci. 618 (2023), https://doi.org/10.1016/j.apsusc.2023.156650.
[103] F. Alduraiei, P. Manchanda, B. Pulido, G. Szekely, S.P. Nunes, Fluorinated thin-film composite membranes for nonpolar organic solvent nanofiltration, Separ. Purif. Technol. 279 (2021), https://doi.org/10.1016/j.seppur.2021.119777.
[104] Y. Sun, T. Sun, J. Pang, N. Cao, C. Yue, J. Wang, X. Han, Z. Jiang, Poly(aryl ether ketone) membrane with controllable degree of sulfonation for organic solvent nanofiltration, Separ. Purif. Technol. 273 (2021), https://doi.org/10.1016/j.seppur.2021.118956.
[105] G. Ma, S. Zhao, Y. Wang, Z. Wang, J. Wang, Conjugated polyaniline derivative membranes enable ultrafast nanofiltration and organic-solvent nanofiltration, J. Membr. Sci. 645 (2022), https://doi.org/10.1016/j.memsci.2021.120241.
[106] X. Zheng, A. Zhou, Y. Wang, X. He, S. Zhao, J. Zhang, W. Li, Modulating hydrophobicity of composite polyamide membranes to enhance the organic solvent nanofiltration, Separ. Purif. Technol. 223 (2019) 211–223, https://doi.org/10.1016/j.seppur.2019.04.078.
[107] K. Chen, P. Li, H. Zhang, H. Sun, X. Yang, D. Yao, X. Pang, X. Han, Q.J. Niu, Organic solvent nanofiltration membrane with improved permeability by in-situ growth of metal-organic frameworks interlayer on the surface of polyimide substrate, Separ. Purif. Technol. 251 (2020), https://doi.org/10.1016/j.seppur.2020.117387.
[108] S. Yuan, J. Swartenbroekx, Y. Li, J. Zhu, F. Ceyssens, R. Zhang, A. Volodine, J. Li, P. Van Puyvelde, B. Van der Bruggen, Facile synthesis of Kevlar nanofibrous membranes via regeneration of hydrogen bonds for organic solvent nanofiltration, J. Membr. Sci. 573 (2019) 612–620, https://doi.org/10.1016/j.memsci.2018.12.047.
[109] Z.-J. Fu, Z.-Y. Wang, M.-L. Liu, J. Cai, P.-A. Yuan, Q. Wang, W. Xing, S.-P. Sun, Dual-layer membrane with hierarchical hydrophobicity and transport channels for nonpolar organic solvent nanofiltration, AIChE J. 67 (4) (2021), https://doi.org/10.1002/aic.17138.
[110] D. Ren, Y.-h. Li, S.-p. Ren, T.-Y. Liu, X.-L. Wang, Microporous polyarylate membrane with nitrogen-containing heterocycles to enhance separation performance for organic solvent nanofiltration, J. Membr. Sci. 610 (2020), https://doi.org/10.1016/j.memsci.2020.118295.
[111] F. Alduraiei, S. Kumar, J. Liu, S.P. Nunes, G. Szekely, Rapid fabrication of fluorinated covalent organic polymer membranes for organic solvent nanofiltration, J. Membr. Sci. 648 (2022), https://doi.org/10.1016/j.memsci.2022.120345.
[112] Y. Xu, S. Yu, G. Peng, A. Sotto, H. Ruan, J. Shen, C. Gao, Novel crosslinked brominated polyphenylene oxide composite nanofiltration membranes with organic solvent permeability and swelling property, J. Membr. Sci. 620 (2021), https://doi.org/10.1016/j.memsci.2020.118784.
[113] B. Li, Y. Cui, T.-S. Chung, Hydrophobic perfluoropolyether-coated thin-film composite membranes for organic solvent nanofiltration, ACS Appl. Polym. Mater. 1 (3) (2019) 472–481, https://doi.org/10.1021/acsapm.8b00171.
[114] P. He, S. Zhao, C. Mao, Y. Wang, G. Ma, Z. Wang, J. Wang, In-situ growth of double-layered polyaniline composite membrane for organic solvent nanofiltration, Chem. Eng. J. 420 (2021), https://doi.org/10.1016/j.cej.2021.129338.
[115] J. Hu, R. Hardian, M. Gede, T. Holtzl, G. Szekely, Reversible crosslinking of polybenzimidazole-based organic solvent nanofiltration membranes using difunctional organic acids: toward sustainable crosslinking approaches, J. Membr. Sci. 648 (2022), https://doi.org/10.1016/j.memsci.2022.120383.
[116] L. Paseta, M. Navarro, J. Coronas, C. Tellez, Greener processes in the preparation of thin film nanocomposite membranes with diverse metal-organic frameworks for organic solvent nanofiltration, J. Ind. Eng. Chem. 77 (2019) 344–354, https://doi.org/10.1016/j.jiec.2019.04.057.
[117] Y. Xu, G. Peng, W. Li, Y. Zhu, Z. Mai, N. Mamrol, J. Liao, J. Shen, Y. Zhao, Enhanced organic solvent nanofiltration of aligned Kevlar composite membrane by incorporated with amino-polystyrene nanospheres, J. Membr. Sci. 647 (2022), https://doi.org/10.1016/j.memsci.2022.120290.
[118] S.-C. Wu, Y. Chen, X. Yan, X.-J. Guo, W.-Z. Lang, ZIF-8 channeled and coordination-bridging two-dimensional WS2 membrane for efficient organic solvent nanofiltration, Chem. Eng. J. 442 (2022), https://doi.org/10.1016/j.cej.2022.136139.
[119] L. Sarango, L. Paseta, M. Navarro, B. Zornoza, J. Coronas, Controlled deposition of MOFs by dip-coating in thin film nanocomposite membranes for organic solvent nanofiltration, J. Ind. Eng. Chem. 59 (2018) 8–16, https://doi.org/10.1016/j.jiec.2017.09.053.
[120] H. Abadikhah, E.N. Kalali, S. Behzadi, S.A. Khan, X. Xu, M.E. Shabestari, S. Agathopoulos, High flux thin film nanocomposite membrane incorporated with functionalized TiO2@reduced graphene oxide nanohybrids for organic solvent nanofiltration, Chem. Eng. Sci. 204 (2019) 99–109, https://doi.org/10.1016/j.ces.2019.04.022.
[121] S. Li, R. Zhang, Q. Yao, B. Su, L. Han, C. Gao, High flux thin film composite (TFC) membrane with non-planar rigid twisted structures for organic solvent nanofiltration (OSN), Separ. Purif. Technol. 286 (2022), https://doi.org/10.1016/j.seppur.2022.120496.
[122] Z.F. Gao, G.M. Shi, Y. Cui, T.-S. Chung, Organic solvent nanofiltration (OSN) membranes made from plasma grafting of polyethylene glycol on cross-linked polyimide ultrafiltration substrates, J. Membr. Sci. 565 (2018) 169–178, https://doi.org/10.1016/j.memsci.2018.08.019.
[123] H. Alhweij, E.A.C. Emanuelsson, S. Shahid, J. Wenk, High performance in-situ tuned self-doped polyaniline (PANI) membranes for organic solvent (nano) filtration, Polymer 245 (2022), https://doi.org/10.1016/j.polymer.2022.124682.
[124] Z. Zhai, C. Jiang, N. Zhao, W. Dong, P. Li, H. Sun, Q.J. Niu, Polyarylate membrane constructed from porous organic cage for high-performance organic solvent nanofiltration, J. Membr. Sci. 595 (2020), https://doi.org/10.1016/j.memsci.2019.117505.
[125] C. Wang, M.J. Park, D.H. Seo, S. Phuntsho, R.R. Gonzales, H. Matsuyama, E. Drioli, H.K. Shon, Inkjet printed polyelectrolyte multilayer membrane using a polyketone support for organic solvent nanofiltration, J. Membr. Sci. 642 (2022), https://doi.org/10.1016/j.memsci.2021.119943.
[126] B.-X. Gu, Z.-z. Liu, K. Zhang, Y.-L. Ji, Y. Zhou, C.-J. Gao, Biomimetic asymmetric structural polyamide OSN membranes fabricated via fluorinated polymeric networks regulated interfacial polymerization, J. Membr. Sci. 625 (2021), https://doi.org/10.1016/j.memsci.2021.119112.
[127] Y. Feng, M. Weber, C. Maletzko, T.-S. Chung, Fabrication of organic solvent nanofiltration membranes via facile bioinspired one-step modification, Chem. Eng. Sci. 198 (2019) 74–84, https://doi.org/10.1016/j.ces.2019.01.008.
[128] Y. Huang, S.-L. Li, Z. Fu, G. Gong, Y. Hu, Preparation of microporous organic solvent nanofiltration (OSN) composite membrane from a novel tris-phenol monomer, Separ. Purif. Technol. 301 (2022), https://doi.org/10.1016/j.seppur.2022.121985.
[129] J. Shen, S. Shahid, A. Sarihan, D.A. Patterson, E.A.C. Emanuelsson, Effect of polyacid dopants on the performance of polyaniline membranes in organic solvent nanofiltration, Separ. Purif. Technol. 204 (2018) 336–344, https://doi.org/10.1016/j.seppur.2018.04.034.
[130] S.K. Das, P. Manchanda, K.-V. Peinemann, Solvent-resistant triazine-piperazine linked porous covalent organic polymer thin-film nanofiltration membrane, Separ. Purif. Technol. 213 (2019) 348–358, https://doi.org/10.1016/j.seppur.2018.12.046.
[131] K. Ma, X. Li, X. Xia, Y. Chen, Z. Luan, H. Chu, B. Geng, M. Yan, Fluorinated solvent resistant nanofiltration membrane prepared by alkane/ionic liquid interfacial polymerization with excellent solvent resistance, J. Membr. Sci. 673 (2023), https://doi.org/10.1016/j.memsci.2023.121486.
[132] Y. Jin, Q. Song, N. Xie, W. Zheng, J. Wang, J. Zhu, Y. Zhang, Amidoxime-functionalized polymer of intrinsic microporosity (AOPIM-1)-based thin film composite membranes with ultrahigh permeance for organic solvent nanofiltration, J. Membr. Sci. 632 (2021), https://doi.org/10.1016/j.memsci.2021.119375.
[133] R. Hardian, K.A. Miller, L. Cseri, S. Roy, J.M. Gayle, R. Vajtai, P.M. Ajayan, G. Szekely, 2D conjugated microporous polymer membranes for organic solvent nanofiltration, Chem. Eng. J. 452 (2023), https://doi.org/10.1016/j.cej.2022.139457.
[134] Y. Li, J. Zhu, S. Li, Z. Guo, B. Van der Bruggen, Flexible aliphatic-aromatic polyamide thin film composite membrane for highly efficient organic solvent nanofiltration, ACS Appl. Mater. Interfaces 12 (28) (2020) 31962–31974, https://doi.org/10.1021/acsami.0c07341.
[135] P. Vandezande, L.E. Gevers, I.F. Vankelecom, Solvent resistant nanofiltration: separating on a molecular level, Chem. Soc. Rev. 37 (2) (2008) 365–405, https://doi.org/10.1039/b610848m.
[136] M. Priske, K.-D. Wiese, A. Drews, M. Kraume, G. Baumgarten, Reaction integrated separation of homogenous catalysts in the hydroformylation of higher olefins by means of organophilic nanofiltration, J. Membr. Sci. 360 (1–2) (2010) 77–83, https://doi.org/10.1016/j.memsci.2010.05.002.
[137] 戴晨哲, 有机溶剂纳滤在精细化工领域中的应用, 膜科学与技术 43 (2023) 144–153.
[138] B. Scharzec, J. Holtkötter, J. Bianga, J.M. Dreimann, D. Vogt, M. Skiborowski, Conceptual study of co-product separation from catalyst-rich recycle streams in thermomorphic multiphase systems by OSN, Chem. Eng. Res. Des. 157 (2020) 65–76, https://doi.org/10.1016/j.cherd.2020.02.028.
[139] J.H. Huang, X.Q. Cheng, Y. Zhang, K. Wang, H. Liang, P. Wang, J. Ma, L. Shao, Polyelectrolyte grafted MOFs enable conjugated membranes for molecular separations in dual solvent systems, Cell Reports Physical Science 1 (4) (2020), https://doi.org/10.1016/j.xcrp.2020.100034.

[140] K.S. Goh, Y. Chen, J.Y. Chong, T.H. Bae, R. Wang, Thin film composite hollow fibre membrane for pharmaceutical concentration and solvent recovery, J. Membr. Sci. 621 (2021), https://doi.org/10.1016/j.memsci.2020.119008.
[141] C. Schnitzer, D. Kruse, M. Lazar, M. Priske, A. Kobus, Die organophile Nanofiltration als neue Grundoperation der Fluidverfahrenstechnik, Chem. Ing. Tech. 86 (5) (2014) 589–593, https://doi.org/10.1002/cite.201300162.
[142] KG Lina Nie1, Yu Wang, Jaewoo Lee, Yinjuan Huang, Realizing small-flake graphene oxide membranes for ultrafast size-dependent organic solvent nanofiltration, Sci. Adv. 6 (2020) 1–12.
[143] Y. Hong, D. Hua, J. Pan, X. Cheng, K. Xu, Z. Huo, G. Zhan, Fabrication of polyamide membranes by interlayer-assisted interfacial polymerization method with enhanced organic solvent nanofiltration performance, Colloids Surf. A Physicochem. Eng. Asp. 663 (2023), https://doi.org/10.1016/j.colsurfa.2023.131075.
[144] Q. Yao, S. Li, R. Zhang, L. Han, B. Su, High-throughput thin-film composite membrane via interfacial polymerization using monomers of ultra-low concentration on tannic acid – copper interlayer for organic solvent nanofiltration, Separ. Purif. Technol. 258 (2021), https://doi.org/10.1016/j.seppur.2020.118027.
[145] S. Darvishmanesh, T. Robberecht, P. Luis, J. Degrève, B. Van der Bruggen, Performance of nanofiltration membranes for solvent purification in the oil industry, J. Am. Oil Chem. Soc. 88 (8) (2011) 1255–1261, https://doi.org/10.1007/s11746-011-1779-y.
[146] G.M. Shi, M.H. Davood Abadi Farahani, J.Y. Liu, T.-S. Chung, Separation of vegetable oil compounds and solvent recovery using commercial organic solvent nanofiltration membranes, J. Membr. Sci. 588 (2019), https://doi.org/10.1016/j.memsci.2019.117202.
[147] X. Lai, C. Wang, L. Wang, C. Xiao, A novel PPTA/PPy composite organic solvent nanofiltration (OSN) membrane prepared by chemical vapor deposition for organic dye wastewater treatment, J. Water Proc. Eng. 45 (2022), https://doi.org/10.1016/j.jwpe.2021.102533.
[148] A.A. Heidari, H. Mahdavi, TFC organic solvent nanofiltration membrane fabricated by a novel HDPE membrane support covered by manganese dioxide/tannic acid-Fe3+layers, J. Taiwan Inst. Chem. Eng. 135 (2022), https://doi.org/10.1016/j.jtice.2022.104363.
[149] S. Li, S. Du, S. Liu, B. Su, L. Han, Ultra-smooth and ultra-thin polyamide thin film nanocomposite membranes incorporated with functionalized MoS2 nanosheets for high performance organic solvent nanofiltration, Separ. Purif. Technol. 291 (2022), https://doi.org/10.1016/j.seppur.2022.120937.